Design and synthesis of click lipids as tools to study immune cell metabolism

Reinalda, L.

Chapter 3

Synthesis and profiling of cyclopropene fatty acid analogues reveal cell type specific uptake in primary immune cells

Introduction

Fatty acids (FAs) play essential roles in every mammalian cell type.[1,2] They serve as structural building blocks of membranes,[3] as fuel to highly energy demanding cells, such as activated immune cells and cancer cells,[4] and as signaling mediators, particularly in immunological processes.[5–8] Identification of the (patho)physiological roles of FAs in immune activation and the shaping and resolution of the immune response is leading to the discovery of new therapeutic targets, such as different free fatty acid receptors (FFARs).[9,10]

FAs used by immune cells can be synthesized *de novo* by the enzymes amino acetyl carboxylase[11] and fatty acid synthase.[12] This *de novo* lipid biosynthesis (DNL) has been studied extensively in recent years as a potential therapeutic target[13] for the treatment of patients with obesity,[14] NAFLD,[15,16] diabetes,[17] tuberculosis,[18] and cancer.[19] Immune cells also take up exogenous FAs to fuel their metabolic and signaling demands. This was long believed to occur via quick passive transport over the cell membrane.[20] However, it was recently reported to be an active process linked to three families of transport proteins: Fatty acid translocase (FAT/CD36),[21–23] the fatty acid-binding proteins (FABPs), and the fatty acid transport proteins (FATPs).[24]

The precise role of each of these receptors in shaping immune function remains to be elucidated for most processes, but it has been shown that specific fatty acids can affect particular aspects of the immune response. For example, exogenous oleic acid, but not palmitoleic acid, is essential for T cell activation and the myeloid suppressor cells in the tumour microenvironment rely heavily on CD36-mediated uptake of palmitic acid for their activation and execution of their immuno-suppressive function.[21,25]

Being able to study the uptake of these individual FAs in immune cells at the single cell level is therefore essential to understand the roles FAs play in shaping the immune response. Fluorophore labeled fatty acid analogs (e.g. BODIPY™-C12/16, TopFluor® oleic acid) were the first reagents to be developed with this aim in mind.[21] They mimic long chain fatty acids by either replacing the end of the hydrophobic tail with, or adding a fluorophore on to it.[26] The approach is live-cell compatible,[27] but the large pendant aromatic fluorophore disrupts the native structure of the fatty acid. This limits their capacity to mimic the uptake of lipids with subtle structural differences.[28]

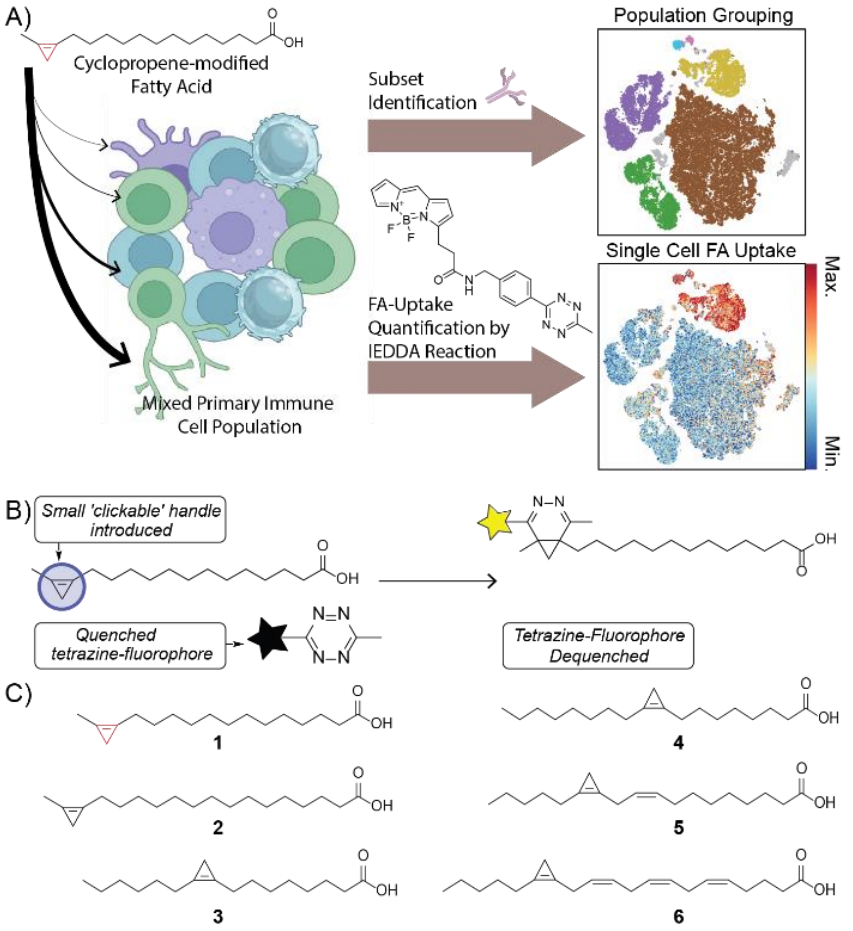

Figure 1. Overview of the approach and synthetic targets. A) Mixtures of primary immune cells are incubated with inverse electron-demand Diels-Alder reactive fatty acids and their uptake quantified with this click reaction. The cells are also stained with an antibody panel to identify subsets. B) IEDDA reaction between CpFA and quenched tetrazine-fluorophore. C) Synthetic CpFA targets.

Bioorthogonal click chemistry has been used to overcome this problem.[29] Instead of using large pendant fluorophores for direct detection, fatty acid analogs bearing the 2-3 atom alkyne and azide groups were developed.[30] These small chemical functionalities allow for fluorophore labeling after completion of the biological time course, whilst keeping structural fidelity to natural FAs.[31] Alkyne analogs of saturated fatty acid (SFA) palmitic acid, and monounsaturated fatty acid (MUFA) oleic acid have, for example, been used to mark differences in the uptake of exogenous FAs in differently polarized bone marrow derived macrophages.[32] They were also employed to show that endothelial cell CD36 controls tissue fatty acid uptake.[23] An alkyne-containing analogue of the ω-3 polyunsaturated fatty acid (PUFA) α-linolenic acid was used to unravel *S. Aureus* capacity to escape antimicrobial FAs.[33] An arachidonic acid analogue was used to reveal the critical role of this PUFA in megakaryocyte differentiation.[34] They have, however not been used to study FA uptake in complex primary immune cell populations.

Whilst the Cu-catalyzed azide-alkyne cycloaddition (CuAAC) is a very powerful approach for labeling lipids, one major downside to the above-mentioned alkyne-modified lipids is that the chemistry required for their labeling requires a toxic copper catalyst. To address this, non-toxic click reactions, such as the strain-promoted azide-alkyne cycloaddition (SPAAC)[35] and the inverse demand Diels-Alder cycloaddition reaction (IEDDA) were developed.[36] A downside, specific to lipid labeling, is that these require either polar groups such as azides and tetrazines, or bulkier bioorthogonal groups, such as cyclooctynes and trans-cyclooctenes, introducing the same steric bulk-problem as for fluorophore-modified lipids.

In search of an alternative to the bulky TCO/BCN the cyclopropene (Cp) stands out. Cps are the smallest strained alkenes that can also react in the IEDDA reaction with electron deficient dienes like tetrazines (Figure 1).[37–39] The cyclopropene is only moderately larger than the alkynes commonly used for fixed-cell FA-labeling and the reaction rate is similar to that of the CuAAC,[36] without the need for a toxic catalyst. This has led to a flurry of activity for using cyclopropenes in chemical biology. Cp-amino acid analogs have been applied to protein labeling,[40–43] nucleotide analogs to label RNA/DNA,[44,45] and carbohydrate analogs for glycan imaging.[38,46–48] Only a few examples of cyclopropenes used in the study of lipid uptake have been reported. Devaraj and co-workers attached a 1,3-cyclopropene tag to the polar head of phospholipids and incorporated those in membranes of a human breast cancer

cell line, which was visualized by confocal microscopy.[37] The van Kasteren group has recently reported the use of the naturally occurring cyclopropene containing lipid sterculic acid,[49] an analog of oleic acid bearing an extra methylene bridging the double bond as a tool for imaging lipid uptake. This lipid could be incorporated in membranes of a dendritic cell line and be used for live-cell imaging and chemical proteomics.[49]

To further assess the potential of using IEDDA reactive Cp-containing lipids, the synthesis and immunological assessment of sterculic acid and five other cyclopropene fatty acid analogs (CpFAs) (Figure 1C, **1** - **6**) of the most abundant long-chain fatty acids50 are described, along with the study of their uptake in complex mixed primary immune cell populations (Figure 1A). Using this method, a well-established phenomenon was confirmed, showing that activated T cells take up more nutrients than naïve T cells.[51] Additionally, it was observed for the first time that different dendritic cell subsets exhibit a higher preference for MUFAs compared to SFAs and PUFAs.

Results and Discussion

Design and Synthesis of Cyclopropene Fatty Acids

It was postulated that for the SFAs palmitic acid and stearic acid, an analogue bearing a terminal methyl cyclopropene with the same carbon chain length would serve as the best possible mimic of the natural FA (Figure 1, Compound **1,2**). The analogue of MUFA palmitoleic acid is based on naturally occurring oleic acid analogue sterculic acid (Figure 1, Compound **3**) where the double bond is replaced by a cyclopropene in the chain extended version of **3** (Figure 1, Compound **4**).[52] In analogs of the ω-6 PUFAs linoleic acid **5** and arachidonic acid **6** the double bond in the ω-6-position is replaced by a cyclopropene, to keep the structural dissimilarity due to the different bond angle minimal.

Various routes towards the synthesis of sterculic acid have been reported, but none to the synthesis of Cp-containing PUFAs.[53–56] Due to the structural similarity of **3** to sterculic acid, the synthetic route of the Cp-palmitoleic acid was based on the most commonly used method: the rhodium-catalyzed [2+1] cycloaddition between a metal carbene formed from ethyl diazoacetate (EDA) and an alkyne (Scheme 1A).[57] The route started with alkylation of 9-decyn-1-ol to yield alcohol **7**. This species was then oxidized with TEMPO / BAIB and

intermediate **8** methylated to yield the methyl ester **9**. Cyclopropene **10** was formed by dropwise addition of EDA to a mixture of rhodium(II)acetate and alkyne **9**. Simultaneous hydrolysis of both esters yielded dicarboxylic acid **11**, which was converted to the bis-acyl chloride prior to decarboxylation with zinc chloride. The resulting cyclopropenium ion intermediate was reduced using $NaBH_4$ under basic conditions, simultaneously reforming the α-carboxylate to yield Cp-palmitoleic acid **3** in 10% yield (2.4% over 5 steps). The most capricious step proved to be the zinc chloride-mediated decarbonylation reaction, with yields ranging from 10 – 40%. This prompted the selection of an alternative strategy for synthesizing the remaining FAs.

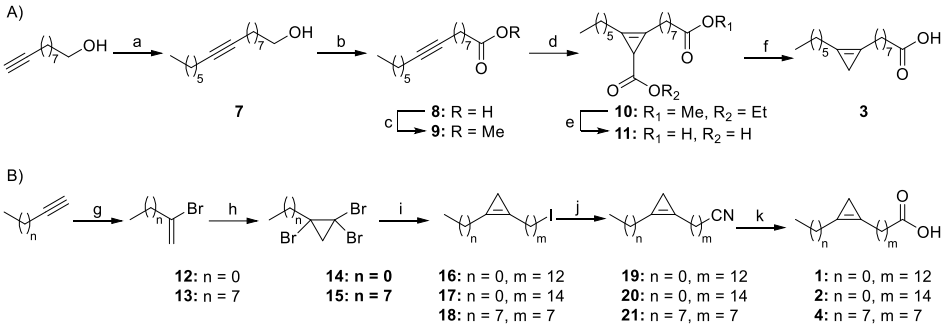

Scheme 1. Synthetic routes towards cyclopropene fatty acids that mimic saturated and monounsaturated fatty acids. A) Route for the synthesis of MUFA analogue **3**. Reagents and conditions: a) *n*-BuLi, 1-bromohexane, NaI, 4:1 THF / HMPA, -78 °C to rt, 18 h, 44% yield. b) TEMPO, BAIB, 2:1 MeCN / water, 0 °C to rt, 2.5 h, 84% yield. c) $SOCl_2$, MeOH, 0 °C, 2.5 h, 88% yield. d) EDA, $Rh_2(OAc)_4$, DCM, 0 °C, 3.5 h, 76% yield. e) KOH, MeOH, reflux, 2.5 h, 97% yield. e) $SOCl_2$, Et_2O, 0 °C, 1 h, then $ZnCl_2$, DCM, rt, 3 h, then $NaBH_4$, NaOH, MeOH, -30 °C to rt, 1 h, 10% yield. B) Adjusted route for the synthesis of SFAs **1**, **2** and MUFA **4**. Reagents and conditions: g) BBr_3, DCM, -78 °C to rt, 3 h, 78% yield. h) NaOH, CTAB, $CHBr_3$, DCM, 0 °C to rt, 18 h, 47% – 57% yield. i) *n*-BuLi, diiodoalkane, THF, -78 °C to 0 °C, 4 h, 27 – 56% yield. j) NaCN, DMSO, 90 °C, 1 h, 68 – 89% yield. k) NaOH, EtOH / water, reflux, 18 h, 37 – 63% yield.

The saturated CpFAs **1** and **2** were synthesized using tribromocyclopropane as a cyclopropene precursor (Scheme 1B).[58] Treatment of that species with two equivalents of *n*-butyllithium (*n*-BuLi) yields a lithiated cyclopropene nucleophile via a double lithium-halogen exchange and an elimination,[59,60] that can be reacted with a diiodoalkane to form the iodocyclopropenes. In the first step, bromination of a terminal alkyne with BBr_3 following Markovnikov's rule yielded bromoalkene **13**. A dibromocarbene-species was formed from bromoform by NaOH in a phase transfer catalytic system, which was reacted with the readily available alkene **12** and compound **13** to give tribromocyclopropanes **14** and **15**. The reaction of the lithiated cyclopropene

nucleophile with an excess of diiodoalkane afforded iodocyclopropenes **16**-**18**. These were converted to nitriles **19**-**21** by reacting them with sodium cyanide followed by basic hydrolysis to give the cyclopropene fatty acids **1**, **2** and **4** in 2.5 – 11.5% yield over 5 steps. Although the yield was still low, the experimental simplicity of the individual steps and higher reproducibility made this the route of choice for the synthesis of compounds **1**, **2** and **4**.

Synthesis of polyunsaturated CpFAs **5** and **6** was first attempted by substitution of 1,2-diiodoethane with the lithiated cyclopropene nucleophile (Scheme S1). This was unsuccessful. A Wittig olefination was therefore chosen to connect the cyclopropene and the unsaturated fatty acid part (Schemes 2A and S2).[61] The route where the aldehyde was introduced on the cyclopropene-containing fragment, was abandoned due to **23** being too unstable for routine synthesis. The inverse approach, where the phosphonium bromide **24** was reacted with fatty ester aldehyde **25** did prove successful (Scheme 2A,B). Alcohol **28** was synthesized by ring-opening of ethylene oxide, catalyzed by $BF_3{\cdot}OEt$ in presence of the lithiated cyclopropene nucleophile from **27**. I had previously found that 1,3-substituted cyclopropene β-alcohols were incompatible with the Appel(-like) reaction. Appel-like conditions using *N*-bromosuccinimide on the 1,2-substituted substrate, however, did afford stable cyclopropene bromide **29** in 59% yield. An overnight substitution reaction with triphenylphosphine under reflux in acetonitrile yielded the target cyclopropene phosphonium bromide **24** in 23% yield over 3 steps. Aldehyde **25** was synthesized in five steps from a diol by protecting the alcohol on one end with a silyl to yield compound **30**, which was oxidized and protected to yield methyl ester **31**. The silyl ether protecting group was removed and the alcohol oxidized affording aldehyde **25**. The phosphorus ylide of **24** was formed *in situ* using NaHMDS and reacted with aldehyde **25** to yield the cyclopropene linoleic methyl ester **34**. Subsequent saponification yielded **5**, to the best of my knowledge the first example of the synthesis of a cyclopropene-containing PUFA analogue.

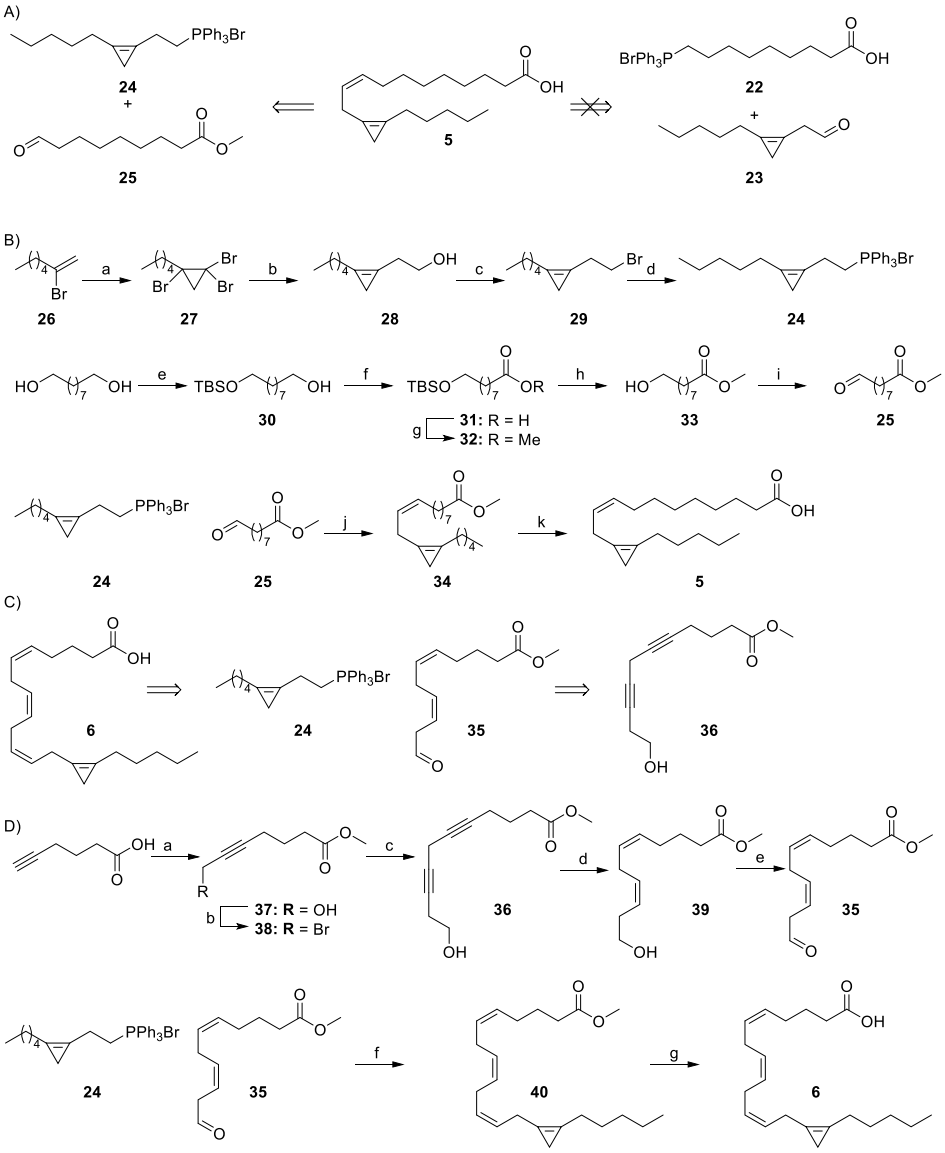

Scheme 2. Optimal synthetic strategy for cyclopropene PUFA analogue synthesis. A) Retrosynthetic analysis of compound **5**. B) Synthetic route towards Cp-linoleic acid **5**. Reagents and conditions: : a) BBr_3, DCM, -78 °C to rt, 3 h, 52% yield. b) *n*-Buli, $BF_3{\cdot}OEt_2$, oxirane, THF, -78 °C to 0 °C, 2 h, 49% yield. c) NBS, PPh_3, DCM, 0 °C to rt, 2 h, 59% yield. d) PPh_3, MeCN, 82 °C, 18 h, 82% yield. e) TBSCl, imidazole, DCM, rt, 3 h, 64% yield. f) TEMPO / BAIB, 2:1 MeCN / water, rt, 3 h, 92% yield. g) MeI, K_2CO_3, DMF, rt, 18 h, 86% yield. h) TBAF, DCM, 0 °C to rt, 5 h, 93% yield. i) DMP, DCM, 0 °C to rt, 1 h, 78% yield. j) NaHMDS, THF, -78 °C to 0 °C, 2.5 h, 44% yield. k) NaOH (aq.), 1:1 THF / EtOH, 70 °C, 2 h, 73% yield. C) Retrosynthetic analysis of **6**. D) Synthetic route towards Cp-arachidonic acid **6**. Reagents and conditions: a) EtMgBr, PFA, THF, 0 °C to 75 °C, 18 h, then: $SOCl_2$, MeOH, 0 °C to rt, 1 h, 51% yield. b) NBS, PPh_3, DCM, 0 C to rt, 1 h, 82% yield. c) CuI,

NaI, K_2CO_3, but-3-yn-1-ol, DMF, rt, 18 h, 72% yield. d) $NaBH_4$, $Ni(OAc)_2 \cdot 4\ H_2O$, ethylenediamine, H_2 (g), MeOH, rt, 2 h, 27% yield. e) DMP, DCM, 0 °C to rt, 1 h, 37% yield. f) NaHMDS, THF, -78 °C to 0 °C, 2.5 h, 54% yield. g) NaOH (aq.), 1:1 THF / EtOH, 70 °C, 2 h, quant. yield.

The synthesis of the arachidonic acid-analogue **6** was next attempted using a Wittig-based sequence (scheme S3). Unfortunately, both the stereoselectivity of the Wittig reactions and the deprotection of the acetal proved troublesome, rendering this approach unfeasible. A route was then designed that employs a Wittig reaction to form the C-C bond between aldehyde **35** and phosphonium bromide **24**, using bis-alkyne **36** as the key intermediate (scheme 2C).[62] Alkynylation of paraformaldehyde with 5-hexynoic acid using an excess of EtMgBr followed by esterification yielded methyl ester **37**, which was converted into the bromide **38** with an Appel-like reaction. Then, a copper(I) mediated cross-coupling with but-3-yn-1-ol afforded skipped diyne **36**. A selective reduction of the alkynes to alkenes was attempted using Lindlar's catalyst. In some cases, cis/trans stereoselectivity issues were encountered, along with frequent overreduction to the alkane before completion. After numerous attempts a different approach using poisoned P-2 Nickel was employed although similar problems were encountered for this reaction.[63,64] For most runs mainly three products were formed, the desired diene and two ene-yne combinations, that could only be purified with HPLC. This approach afforded diene **39** with complete Z-selectivity. A Wittig reaction between aldehyde **35** and phosphonium bromide **24** yielded cyclopropene arachidonyl methyl ester **40** that could be saponified to yield **6** (Scheme 2D).

Optimization of Ex-Vivo Uptake of CpFAs in Mouse Splenocytes

With a library of six cyclopropene fatty acid analogs of FAs **1** - **6** that play key roles in shaping the immune response,[65,66] the suitability of these analogs to study fatty acid uptake in immune cell populations was next assessed. Previous work demonstrated that sterculic acid could be used to study fatty acid uptake in a dendritic cell line.[49] To investigate whether CpFAs **1** - **6** could be utilized to study nutrient uptake in other immune cells, their uptake by primary splenocytes, obtained through mechanical homogenization of mouse spleens, was examined. They contain a mixture of many key immune cells in various states of activation of which the flow cytometric identification with well-characterized antibodies is routinely performed.[67,68]

After pulsing splenocytes with the CpFAs **1** - **6**, uptake was first assessed by performing the click reaction with tetrazine-AF488. All six CpFAs showed active uptake at 37 °C compared to cells that were incubated with CpFAs on ice as a negative control (Figure S1A,B). However, notable background was detected in the ice-control cells for all compounds. To optimize detection, the levels of CpFA were titrated using sterculic acid, which had been characterized previously, or by adjusting the concentration of tetrazine-AF488 (Figure 2A-C). The concentration of tetrazine had the largest impact on detection levels, as performing the reaction without CpFA treatment led to a high background fluorescence (Figure 2B). To resolve the high non-specific binding of the tetrazine-AF488 **41**, tetrazine-BODIPY FL **42** (Figure 2A,D) was tested as an alternative, which is quenched until reaction with an alkene (Figure 2D-F).[49] Using this method, the background of the click reaction in the absence of CpFAs was comparable to splenocytes with no reaction performed (Figure 2E), and similar fluorescence values were calculated for both tetrazine-conjugates after background subtraction (Figure 2C, F). Importantly, the same uptake pattern was observed for both the reaction with tetrazines **41** and **42** across specific immune cell populations (Figure S1B). The improved signal-to-noise ratio as indicated by the calculated stain-index, however, makes the BODIPY more suitable for flow-cytometry based assays (Figure S1C). Moving forward, a cpFA concentration of 25 µM of CpFA was chosen, which falls in the range of physiological concentration for all parent lipids,[69] and 1 µM of tetrazine-BODIPY FL to prevent risk of fluorescent spillover.

One factor to consider in these assays, is the potential difference in dequenching upon reaction of BODIPY FL with each of the CpFAs. This was assessed by performing an *in vitro* fluorescence turn-on assay where the six CpFAs (25 µM) were incubated with tetrazine-BODIPY FL (1 µM) in PBS for 30 min and the fluorescent signal (λ_{ex} = 447 nm, λ_{em} = 530 nm) measured (Table S2) to create an adjusted value (relative to linoleic acid). Applying the adjusted values to the intensities of pulsed splenocytes did not alter the overall pattern of uptake across CpFAs (Figure S1E).

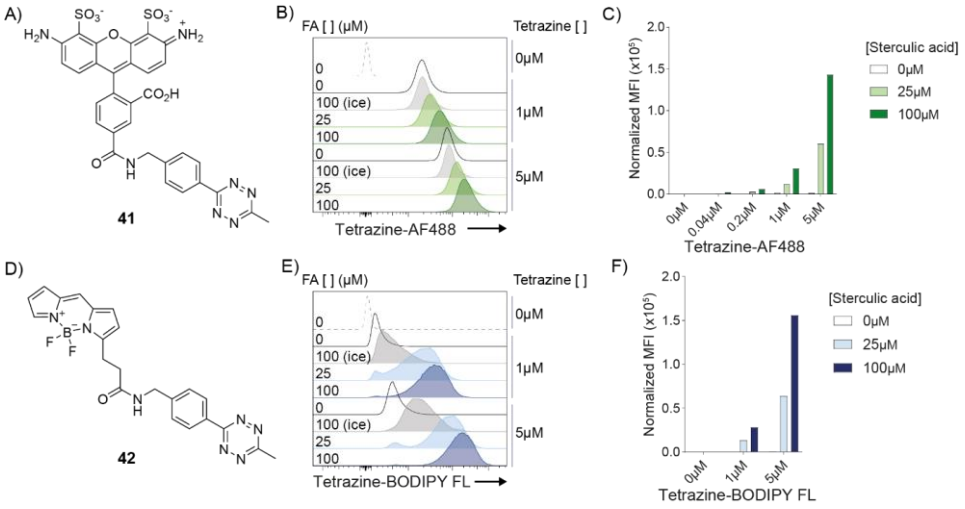

Figure 2. Optimization of ex-vivo uptake of sterculic acid 4 in mouse splenocytes. Splenocytes were incubated with sterculic acid (0, 25 or 100 μM) for 30 minutes prior to fixation and subsequent click-reaction with either AF488-tetrazine (0.04, 0.2, 1 or 5 μM) or BODIPY-tetrazine (0, 1 or 5 μM). A, D) Chemical structures of AF488-tetrazine 41 and tetrazine-BODIPY FL 42. B) Histograms of signal after uptake. Green: 37 °C, grey: cold control. C) Bar chart of the data shown in B. E) Signal resulting from reaction between 4 after uptake and tetrazine-BODIPY FL 42. Green: 37 °C, grey: cold control . F) Bar chart of the data shown in E. Data shown in this figure represents uptake performed in splenocytes harvested from individual mice (N = 3) with no technical replicates (n = 1).

To evaluate the suitability of CpFAs **1** - **6** as analogs, a competition assay was performed in which CpFAs (25 μM) were simultaneously pulsed with 25, 50, or 100 μM of the parent fatty acid (Figure S1F).Competition of palmitic acid and arachidonic acid were complete (i.e. only 20% of signal remained in presence of 100 μM of the parent lipid). Uptake inhibition of stearic acid, palmitoleic acid, oleic acid and linoleic acid was not complete, with 40% to 70% of signal remaining in presence of 100 μM of the parent lipid, comparable to that of alkyne FAs.[70] This suggests that either uptake at 125 μM is not saturated for these lipids, or that CpFAs **2-5** are only partial mimics of the parent lipids. Cell viability was not affected by the presence of the CpFAs, as determined by staining with a live exclusion dye following uptake, which was detected by flow cytometry (Figure S1D).

Single Cell Studies of FA Uptake in a Complex Immune Cell Population

The optimized protocol was then applied to the all six CpFAs **1** - **6**. Again, all compounds showed active uptake at 37 °C that was reduced when cells were

left on ice (Figure 3A,B). With the protocol optimized and the CpFAs validated as analogs for their native counterparts, the focus shifted to determining how fatty acids are differentially utilized across immune populations from the mouse spleen. Following the uptake assay and click reaction, cells were stained using fluorescent-conjugated antibodies targeting receptors unique to specific immune populations, allowing their identification by flow cytometry.

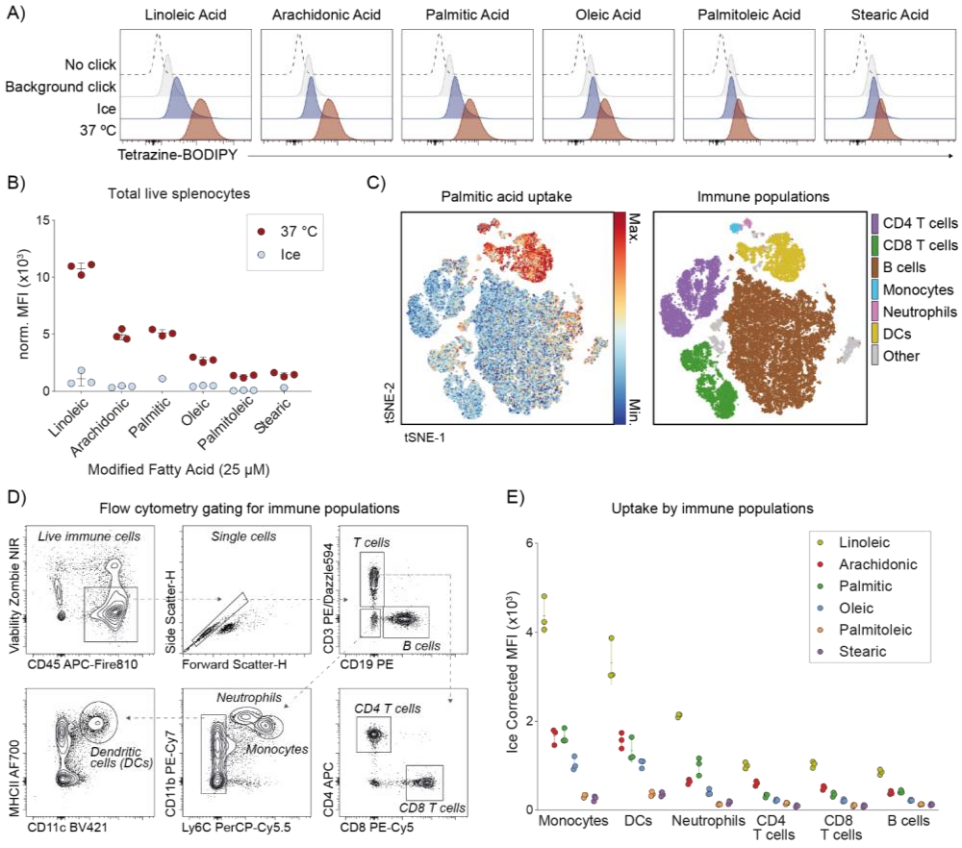

Figure 3. Uptake of CpFA library 1-6 in splenocytes. A) Representative histograms of the uptake of six CpFAs (37 °C) including autofluorescence (No click), non-specific binding of tetrazine-BODIPY FL (Background click) and passive uptake (ice). B) Change in normalized MFI of CpFA (25 µM) uptake with cold control included. C) Dimensionality reduction using tSNE was performed on splenocytes for Cp-palmitic acid uptake. Right panel shows splenocytes population including CD19+/CD3 B cells, CD11b+/Ly6Chi monocytes, Ly6Chi neutrophils, CD3+/CD19 CD4+ T cells, CD3+/CD19 CD8+ T cells and MHCII+/CD11c+ dendritic cells. Bottom panel shows the corresponding Cp-palmitic acid uptake. D) Corresponding manual gating strategy. E) Change in for passive uptake corrected MFI of CpFA uptake in different immune cell subsets. Data shown in this figure represents uptake performed in splenocytes harvested from individual mice (N = 3) with no technical replicates (n = 1).

To assess which immune cells take up the various FAs, an unsupervised dimensional reduction was performed to visualize the correlation between immune cell type and FA uptake, using palmitic acid as an example (Figure 3C). The resulting t-distributed Stochastic Neighbour Embedding (tSNE) plot indicated particularly high uptake in cells from the myeloid lineage, including monocytes and dendritic cells, whereas lymphoid cells, such as T and B cells, demonstrated comparatively low uptake. These findings were confirmed by manually gating and determining the detection of CpFA for each major immune subset according to Figure 3D, and found a similar pattern of uptake for all FA species tested across the different cell types (Figure 3E). Phagocytes, the major cells of innate immunity like monocytes, neutrophils and DCs have a high expression of CD36 compared to T and B cells, which could perhaps explain a higher FA uptake.[71,72] Notably, all immune cells showed a preference for the PUFAs, Cp-linoleic and Cp-arachidonic acid, followed by the SFA Cp-palmitic acid. Therefore, the library of novel CpFAs has the potential to reveal specific needs for particular fatty acid species across diverse primary immune cell populations.

FA uptake in immune cells is rapidly regulated during activation, or within the same cell type can differ depending on their functional state. $CD4^+$ T cells, for instance, quickly increase their need for environmental FA when stimulated by the matched antigen to their specific T cell receptor, allowing them to divide and produce effector molecules. Expression of the T cell activation marker CD44 appeared to correlate with palmitic acid uptake, which was further confirmed with manual gating and analysis (Figure 4A,B). Indeed, all analogs showed an increase in uptake in activated compared to naïve $CD4^+$ T cells, however this was less evident for palmitoleic and stearic acid (Figure 4C). Uptake in type 1 and type 2 conventional dendritic cells (cDC1 and cDC2, respectively) was also compared. cDC1s have specialized functions in activating cytotoxic $CD8^+$ T cells, and cDC2s in activing helper $CD4^+$ T cells.[73] Although both cells had relatively comparable uptake for most FA species, cDC2 generally trended towards more FA uptake than cDC1 (Figure 4F). Interestingly, cDC2 did show a particular significant difference in MUFA uptake compared to cDC1, indicating cDC1 and cDC2 may have distinct FA requirements (Figure 4D,E). Altogether, this data demonstrate that the library of clickable-FA can be applied to biological systems to provide novel insights into the diverse metabolic requirements of cells depending on their lineage or activation state, here using immune cells as a key example.

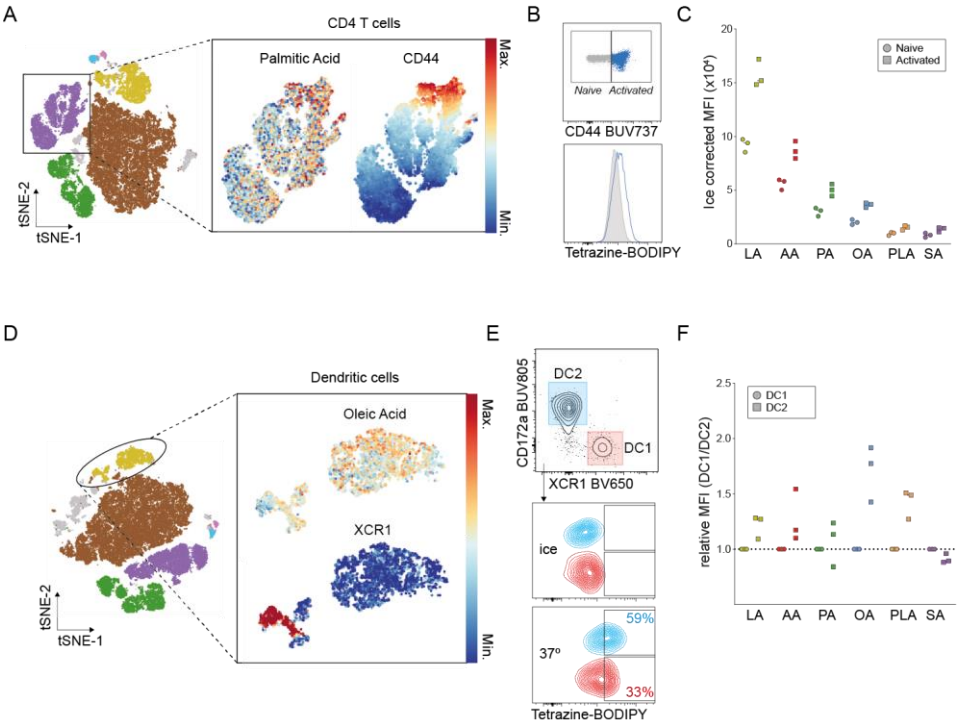

Figure 4. A) Dimensionality reduction using tSNE on CD4⁺ T cells expressing activation marker CD44 for Cp-palmitic acid uptake. B) Top panel shows the manual gating strategy for naïve CD44⁻ T cells and activated CD44⁺ T cells, bottom panel the representative histogram. C) Difference in corrected MFI of CpFA uptake between naïve and activated T cells. D) Dimensionality reduction using tSNE on dendritic cells expressing defining markers XCR1 (cDC1) and CD172a (cDC2) for Cp-oleic acid uptake. E) Manual gating strategy on ice to correct for passive uptake (middle) and at 37 °C (bottom) of CD11C⁺/MHCII⁺ CD172a⁻ cDC1s and CD11C⁺/MHCII⁺ CD172a⁺ cDC2s(top). F) Fold change CpFA uptake (gMFI) relative to mean cDC1 expression per CpFA as gated in (E). Data shown in this figure represents uptake performed in splenocytes harvested from individual mice (N = 3) with no technical replicates (n = 1).

Conclusion

This study reports the use of a cyclopropene long chain fatty acid analog library, covering the three main types of saturation, to investigate fatty acid uptake of individual immune cells in complex cell populations. An optimized synthetic method was applied to synthesize SFA and MUFA analogs and new synthetic methodology was developed to produce the first-ever reported cyclopropene PUFA analogs. An initial uptake experiment revealed a high background when using tetrazine-AF488 due to non-specific binding. Hence,

the quenched tetrazine-BODIPY FL was employed, resulting in much better resolution, yet requiring correction for the difference in turn-on ratio for the different fatty acid-BODIPY FL conjugates. The uptake of palmitic acid was visualized in a tSNE plot revealing a higher FA uptake for cells from the myeloid, for instance monocytes and dendritic cells, compared to lymphoid cells like T and B cells. Within all different immune cell types a similar pattern was observed where immune cells have a preference for PUFAs, followed by SFA palmitic acid and MUFA oleic acid. Furthermore, it was shown that different cell states (e.g. activated or naïve T cells) lead to a quantitative change in exogenous FA uptake and that different subsets of immune cells exhibit different preferences for FA uptake (e.g. cDC1 require less MUFA then cDC2). This established a platform which can be applied to study relationships between nutrient uptake and immune cell function on a new level.

Acknowledgement

Graham Heieis is gratefully acknowledged for his guidance, performing most of the uptake studies and processing the data. Jeroen Duijn is thanked for the synthesis of some building blocks. Jeroen punt and Wouter Driever are kindly acknowledged for their valuable discussions on the synthesis of some of the difficult intermediates. Kristine Bertheussen is kindly acknowledged for sharing her knowledge on working with sterculic acid in live cells.

Supporting Schemes and Figures

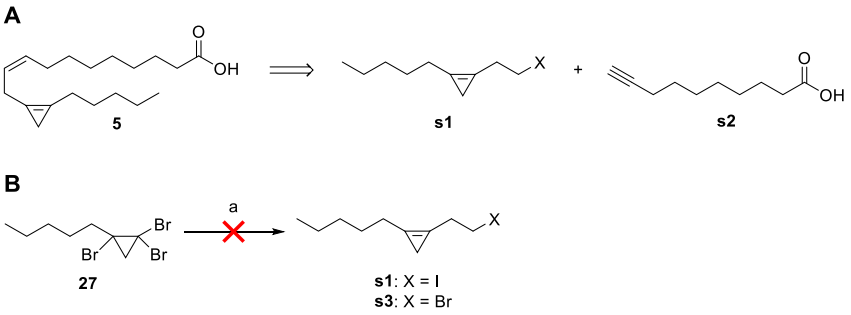

Scheme S1. Synthetic strategy for PUFA synthesis. A) Retrosynthetic analysis of compound 5. B) Attempted route to form cyclopropene halides s1 or s3. Reagents and conditions: a) *n*-Buli, THF, 1,2-diiodoethane or 1-bromo-2-iodoethane, -78 °C to 0 °C, 4 h.

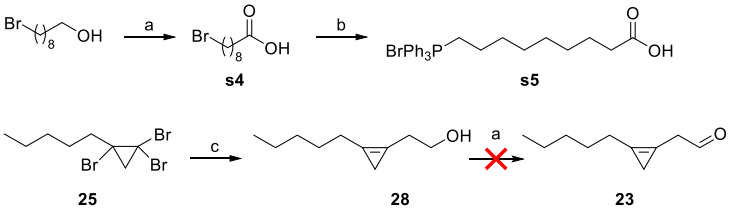

Scheme S2. Synthetic route for phosphonium bromide s5 and attempted route towards cyclopropene aldehyde 23. Reagents and conditions: a) TEMPO, BAIB, 2:1 MeCN / water, rt, 4h, 94% yield. b) PPh_3, MeCN, reflux, 18 h, quant. yield. c) *n*-Buli, $BF_3{\cdot}OEt_2$, oxirane, THF, -78 °C to 0 °C, 2 h, 49% yield. d) DMP, DCM, 0 °C to rt, 2 h. OR DMSO, $C_2O_2Cl_2$, DCM, Et_3N, -78 °C to rt, 2 h. OR DMSO, Ac_2O, DCM, rt, 2 h.

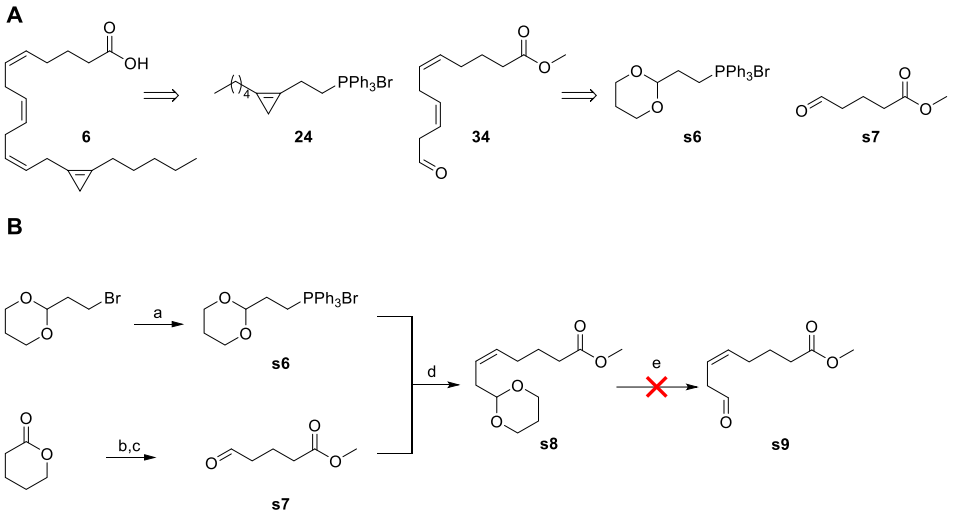

Scheme S3. Synthetic strategy for PUFA with 3 or more double bonds. A) Retrosynthetic analysis of fatty acid **6**. B) Reagents and conditions: a) PPh_3, MeCN, 82 °C, 18 h, 15% yield. b) H_2SO_4, MeOH, reflux, 18 h, 72% yield. c) DMP, DCM, 0 °C to rt, 2 h, 40% yield. d) NaHMDS, THF, -78 °C to rt, 2 h, 65% yield (95% Z-config.). e) HCl (aq.), THF, rt, 20 min OR AcOH, water, 85 °C, 4 h

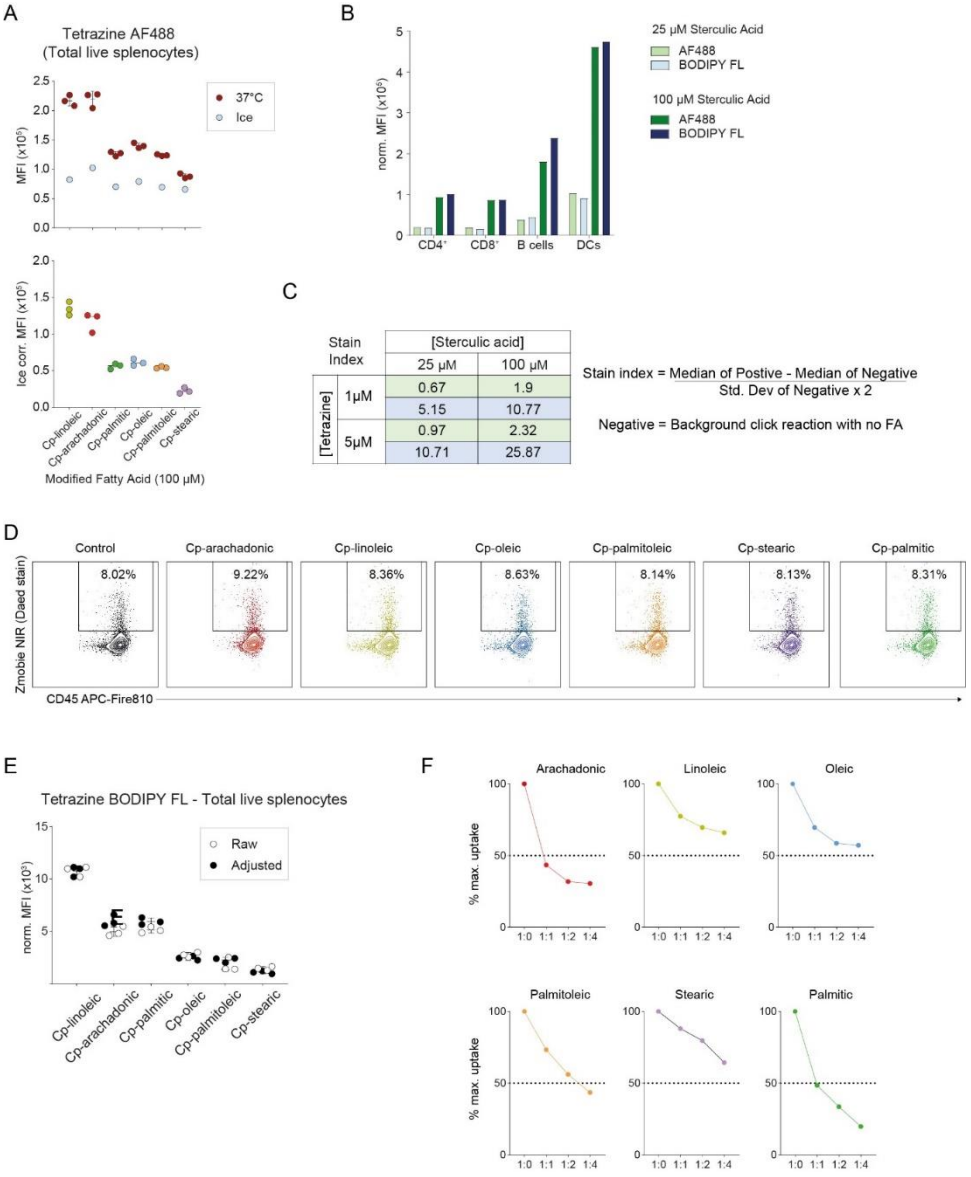

Figure S1. Supporting Figure on the application of Cp-FAs in splenocytes. A) Median fluorescent intensity of Tetrazine-AF488 (5 µM) following click reaction with 100 µM cpFA pulsed splenocytes (top) and normalized values after subtracting the MFI for splenocytes pulsed on ice (bottom). B) Ice-subtracted MFI of immune populations from the spleen, using 1 µM of either tetrazine-AF488 or tetrazine-BODIPY FL. C) The estimated stain index for tetrazine-AF488 (green) or tetrazine-BODIPY FL (blue), calculated as shown. D) Frequency of dead cells within the CD45+ single cell population, determined by amine dye exclusion and flow cytometry, following cpFA pulse (25 µM). E) Raw and adjusted data for each cpFA according to relative fluorescent intensity in a cell-free assay, set relative to linoleic acid. F) Competition assay showing the relative cpFA uptake with increasing concentration of the corresponding native FA.

Experimental section

Immunology

Ethical statement

All experiments were performed in accordance with the Institute for Laboratory Animal Research Guide for the Care and Use of Laboratory Animals or had received approval from the Ethical Review Board for Animal Experimentation of the Leiden University Medical Center, Leiden, the Netherlands.

Isolation of splenocytes

Spleens were isolated from naïve C57BL/6 mice bred under specific pathogen free (SPF) conditions. To obtain a single cell suspension, spleens were minced with scissors in a 2 mL Eppendorf and shaken at 37 °C, 200 rpm for 30 minutes in 1 mg/mL of Collagenase IV reconstituted in RPMI medium. Tissue digestion was stopped by adding 1 mL of cold PBS containing 0.5% BSA and 2 mM EDTA and placed on ice. The remaining homogenate was crushed and washed through a 40 µM strainer into a 50 mL tube, spun at 400g for 5 minutes and resuspended in 3 mL of ACK lysis buffer to remove red blood cells. After 5 minutes in lysis solution, 7 mL of cold PBS was added and cells were spun, washed through a second 40 µM strainer and counted for plating using a hemocytometer.

Preparation of fatty acid stocks

Solid cpFA stocks were first constituted in DMSO to make a 50 mM solution. Two 10x Step-wise dilutions were then done in RPMI medium containing 0.5% fatty acid free BSA to make a 5 mM and subsequent 0.5 mM working stock. The 0.5 mM stock was then diluted to the appropriate 1x concentration to be added to isolated splenocytes.

Uptake assay

Working FA stocks were first pre-warmed in a 37 °C water bath. 1-2 x 10^6 splenocytes were plated in a 96-well V-bottom plate and kept on ice. Plated cells were washed twice in 200 µL of cold PBS. After washing, 100 µL of pre-diluted FA stocks (in the appropriate ratio with native FA for the competition experiment) were added directly to the splenocytes, which were immediately

re-suspended by gentle pipetting. Resuspended cells were either placed in a 37 °C 5% CO_2 incubator or left on ice for 30 minutes, followed by addition of 100 µL cold PBS (0.5% BSA, 2mM EDTA) and spun at 400g for 5 minutes. Cells were washed an additional 2 times with cold PBS and left on ice for cell staining.

Cell staining and click-reaction for flow cytometry

Following FA uptake, splenocytes were stained in 50 µl of Zombie NIR viability dye diluted 500x and anti-XCR1 antibody in PBS for 15 minutes at room temperature. Cells were then washed 2x with 150 µL of cold PBS (0.5% BSA, 2mM EDTA), fixed with 2% methanol-free formaldehyde for 10 minutes at room temperature, and washed twice with PBS. Cells were subsequently permeabilized by incubation in 50 µL of PBS containing 0.1% saponin and 1% BSA for 15 minutes. Permeabilized cells were washed with PBS and the tetrazine-cyclopropene click reaction was performed by diluting the indicated tetrazine-fluorophore in PBS and incubating in 50 µL at room temperature for 1 hour in the dark. Cells were washed 2 times in PBS and either left in the fridge until staining could be performed or immediately stained with 50 µL of antibody cocktail for the remaining surface markers for 30 minutes, washed twice with PBS, and resuspended in 150 µL PBS for acquisition. A full list of antibodies used can be found in Supplementary Table S1. Fully stained samples were acquired on a Cytek 5-laser Aurora and unmixed using SpectroFlo v3. Analysis was done using FlowJo v10, GraphPad Prism and OMIQ.ai.

Fluorescence assay

cpFA stocks were diluted to 50 µM in a similar way to the uptake assay. In a black 96-well flat-bottom plate, 100 µL of tetrazine-BODIPY FL (2 µM) was added to 100 µL of cpFA stock (50 µM) and left to react at room temperature for 1 hour. The plate was scanned for fluorescence on a CLARIOstar plate reader (BMG LABTECH) with excitation/emission at 477-14/530- 40 and dichroic filter 497 showing the turn-on ratio between the sample and negative control (1 µM tetrazine-BODIPY FL), as an average of the three samples.

Table S4. Flow cytometry reagents.

Marker	Conjugate	Dilution	Supplier	Cat. #
CD45	APC-Fire810	1000x	BioLegend	103174
CD3	PE/Dazzle594	1000x	BioLegend	100246
CD4	APC	1000x	ThermoFisher	17-0042-83
CD44	BUV737	1000x	BD Biosciences	612799

CD8	PE-Cy5	1000x	ThermoFisher	15-0081-82
CD19	PE	200x	ThermoFisher	12-0191-82
MHCII	AF700	400x	ThermoFisher	56-5321-82
CD11c	BV421	400x	BioLegend	117330
XCR1	BV650	400x	BioLegend	148220
CD172a	BUV805	200x	BD Biosciences	741997
CD11b	PE-Cy7	10000x	ThermoFisher	25-0112-82
Ly6C	PerCP-Cy5.5	1000x	BioLegend	128028

Table S5. Turn-on Ratio of cpFAs in fluorescence assay with tetrazine-BODIPY FL.

cpFA	**Turn-on Ratio**	**Relative ToR**
Cp-palmitic acid	4.9	0.56
Cp-stearic acid	1.8	1.58
Cp-palmitoleic acid	5.3	0.52
Cp-oleic acid	2.2	1.29
Cp-linoleic acid	2.8	1
Cp-arachidonic acid	3.2	0.88

Chemistry

General information

All commercially available reagents and solvents were used as received unless stated otherwise. Anhydrous solvents were prepared by storage over activated 3 Å (only for MeOH) or 4 Å molecular sieves. Reaction progress was determined with thin layer chromatography (TLC) (Sigma, TLC Silica gel 60 F254) via UV visualisation (λ = 254 nm) and potassium permanganate stain (6 g $KMnO_4$ and 40 g, K_2CO_3 in 600 mL water). All column chromatography purifications were performed using solvents as received and silica gel (Macherey-Nagel, Kieselgel 60 M, 0.04 – 0.63 mm). Analytical LC-MS analysis was performed on a Finnigan Surveyor HPLC system (detection at 200-600 nm) with an analytical C18 column (Gemini, 50 x 4.6 mm, 3 µm particle size, Phenomenex) coupled to a Thermo LCQ Fleet Ion mass spectrometer (ESI+). Solvent system: A: water (gradient, 10-90%), B: CH_3CN (gradient, 90-10%), C: (constant, 10%) 1% TFA (aq). Recorded data was interpreted and analysed using Xcalibur software. ^{1}H and ^{13}C NMR spectra were recorded using a Brüker AV-400 (400/101 MHz) or AV-500 (500/126 MHz). Chemical shift values are

reported in ppm (δ) relative to the residual solvent signal of $CDCl_3$ (δ = 7.26 ppm for ^1H and δ = 77.16 ppm for ^{13}C NMR). Multiplicities are given as singlet (s), doublet (d), triplet (t), quartet (q), pentet (p), doublet of doublets (dd), broad singlet (br s) and multiplet (m). Recorded data was interpreted and analysed using MestReNova software.

General procedure A: Oxidation of alcohol to carboxylic acid

(Diacetoxyiodo)benzene (3 eq) and TEMPO (0.3 eq) were added to a solution of the alcohol (1 eq) in 2:1 MeCN / water (0.2 M) at 0 °C and stirred for 3 h at rt. The solution was quenched with sat. aq. $Na_2S_2O_3$, diluted with water and extracted with EtOAc (3x). The combined organic layers were washed with brine, dried over $MgSO_4$ and concentrated under reduced pressure. The crude product was purified by silica gel column chromatography to afford the carboxylic acid.

General procedure B: Hydrobromination of alkyne

In a slightly modified procedure from the literature,[74] terminal alkyne (1 eq) was added dropwise to a diluted solution of BBr_3 (0.5 M in anh. DCM) (0.5 eq) at -78 °C under N_2 atmosphere and the reaction was slowly warmed to rt and stirred for 3 hours. The solution was cooled to 0 °C and acetic acid (30 eq) was added and stirred for another 1 h. The solution was neutralized carefully with sat. aq. $NaHCO_3$ and extracted with DCM (3x). The combined organic layers were washed with brine, dried over $MgSO_4$ and concentrated under reduced pressure (900 mbar). The crude product was purified by silica gel column chromatography (pentane) to afford 2-bromoalkene.

General procedure C: Cyclopropanation of 2-bromoalkene

In a slightly modified procedure from the literature,[58] a sat. aq. NaOH solution (5 eq) was added dropwise to a solution of 2-bromo alkene (1 eq) and cetyltrimethylammonium bromide (0.1 eq) in bromoform (3 eq) and DCM (1.0 M) at 0 °C and stirred for 18 h. The solution was diluted with water and extracted with DCM (3x). The combined organic layers were washed with brine, dried over $MgSO_4$ and concentrated under reduced pressure. The crude product was purified by silica gel column chromatography (pentane) to afford the tribromocyclopropane.

General procedure D: Substiution of tribromocyclopropane on diiodide

In a slightly modified procedure from the literature,[75] a solution of *n*-butyllithium (2.2 eq) was added dropwise to a solution of tribromocyclopropane (1 eq) in anhydrous THF (0.25 M) at -78 °C under N_2 atmosphere and was slowly warmed to 0 °C and stirred for 1 hour. A solution of diiodoalkane (2 eq) in anhydrous THF (1.0 M) was added and the reaction was stirred for 3 h at rt. The reaction was quenched with water, extracted with 1:1 Et_2O / pentane (3x). The combined organic layers were washed with brine, dried over $MgSO_4$ and concentrated under reduced pressure. The crude product was purified by silica gel column chromatography (pentane) to afford the iodocyclopropene.

General procedure E: Substitution of nitrile on iodocycloprrpene

In a slightly modified procedure from the literature,[74] NaCN (2 eq) was added in one portion to a solution of iodocyclopropene (1 eq) in anhydrous DMSO (0.2 M) under N_2 atmosphere and stirred at 90 °C for 1 h. The reaction was diluted with water and extracted with Et_2O (3x). The combined organic layers were washed with brine, dried over $MgSO_4$ and concentrated under reduced pressure. The crude product was purified by silica gel column chromatography (Et_2O/pentane 1:9) to afford the nitrilecyclopropene.

General procedure F: Hydrolysis of nitrilecyclopropene

In a slightly modified procedure from the literature,[74] a sat. aq. NaOH solution (10 eq) was added to a solution of nitrilecyclopropene (1 eq) in 2:1 EtOH / water (0.2 M) and refluxed overnight. The reaction was acidified with aq. 1 M HCl and extracted with Et_2O (3x). The combined organic layers were washed with brine, dried over $MgSO_4$ and concentrated under reduced pressure. The crude product was purified by silica gel column chromatography (Et_2O/pentane 1:9, 1% AcOH) to afford the cyclopropene fatty acid.

General procedure G: Synthesis of phosphonium bromides

In a slightly modified procedure from the literature,[76] triphenylphosphine (1.1 eq) was added to a solution of alkylbromide (1 eq) in anh. MeCN at rt under N_2 atmosphere and the reaction mixture was stirred for 18 h at 100 °C. The solvents were removed under reduced pressure and the crude product was purified by silica gel column chromatography (DCM/MeOH 99:1 to 19:1) to afford the phosphonium bromide.

General procedure H: Hydrolysis of cyclopropene fatty acid methyl ester

An aq. 2 M NaOH solution (5 eq) was added to a solution of protected cyclopropene fatty acid methyl ester (1 eq) in 1:1 THF / EtOH (0.2 M) and stirred at 70 °C for 2 h. The reaction mixture was acidified with aq. 1 M HCl and extracted with Et_2O (3x). The combined organic layers were washed with brine, dried over $MgSO_4$ and concentrated under reduced pressure. The crude product was purified by silica gel column chromatography (Et_2O/pentane 1:9, 1% AcOH) to afford the cyclopropene fatty acid.

hexadec-9-yn-1-ol (7)

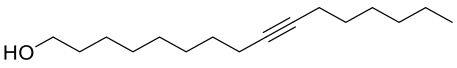

In a slightly modified procedure from the literature,[77] *n*-BuLi (2.5 M in hexanes, 8.80 mL, 22 mmol, 2.2 eq) was added dropwise to a solution of dec-9-yn-1-ol (1.54 g, 10.0 mmol, 1 eq) in 4:1 THF / HMPA (0.1 M) at -78 °C under N_2 atmosphere and the reaction mixture was stirred for 1 h gradually warming to rt. The formed suspension was cooled back to -78 °C, 1-bromohexane (1.35 ml, 9.6 mmol, 0.96 eq) and NaI (75 mg, 0.50 mmol, 0.05 eq) were added dropwise and the reaction was stirred for 18 h slowly warming to rt. The solution was quenched with water and extracted with 1:1 diethyl ether / pentane (3x). The combined organic layers were washed with brine, dried over $MgSO_4$ and concentrated under reduced pressure. The crude product was purified by silica gel column chromatography (Et_2O / pentane 1:19 to 1:9) to afford compound **7** (1.04 g, 4.38 mmol, 43.8 % yield) as a colorless oil. **^{1}H NMR** (400 MHz, $CDCl_3$) δ 3.47 (t, *J* = 6.8 Hz, 2H), 3.22 (s, 1H), 2.02 (t, *J* = 7.0 Hz, 4H), 1.56 – 1.09 (m, 20H), 0.78 (t, *J* = 7.0 Hz, 3H). ^{13}C NMR (101 MHz, $CDCl_3$) δ 80.1, 80.0, 62.4, 32.6, 31.3, 29.4, 29.1, 29.1, 29.1, 28.8, 28.5, 25.7, 22.5, 18.7, 18.7, 14.0.

hexadec-9-ynoic acid (8)

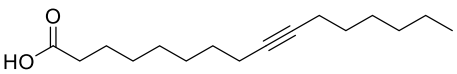

General procedure A was used with compound **7** (402 mg, 1.69 mmol, 1.0 eq) as starting material, the crude product was purified by silica gel column chromatography (Et_2O / pentane 1:9) to afford compound **8** (357 mg, 1.41 mmol, 84% yield) as a light yellow crystalline solid. **^{1}H NMR** (400 MHz, $CDCl_3$) δ 2.33 (t, *J* = 7.5 Hz, 2H), 2.12 (t, *J* = 6.6 Hz, 4H), 1.69 – 1.57 (m, 2H), 1.51 – 1.17 (m, 16H), 0.87 (t, *J* = 6.9 Hz, 3H). **^{13}C NMR** (101 MHz, $CDCl_3$) δ 180.6, 80.4, 80.1, 34.2, 31.5, 29.2, 29.2, 29.1, 28.9, 28.7, 28.7, 24.7, 22.7, 18.9, 18.8, 14.2. Spectral data was in accordance with the literature.[78]

methyl hexadec-9-ynoate (9)

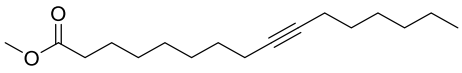

Thionylchloride (0.41 mL, 5.65 mmol, 4.0 eq) was added to a solution of compound **8** (357 mg, 1.41 mmol, 1.0 eq) in methanol (0.2 M) at 0 °C under nitrogen atmosphere and stirred for 2.5 h at rt. The reaction mixture was concentrated under reduced pressure and the crude product was purified by silica gel column chromatography (Et_2O / pentane 1:49) to afford compound **9** (333 mg, 1.25 mmol, 88% yield) as a clear oil. **^{1}H NMR** (300 MHz, $CDCl_3$) δ 3.62 (s, 3H), 2.26 (t, *J* = 7.5 Hz, 2H), 2.13 – 2.04 (m, 4H), 1.65 – 1.51 (m, 2H), 1.49 – 1.15 (m, 16H), 0.85 (t, *J* = 6.7 Hz, 3H). **^{13}C NMR** (75 MHz, $CDCl_3$) δ 174.3, 80.4, 80.1, 51.4, 34.1, 31.5, 29.2, 29.1, 29.1, 28.9, 28.7, 28.6, 25.0, 22.7, 18.8, 18.8, 14.1

ethyl 2-hexyl-3-(8-methoxy-8-oxooctyl)cycloprop-2-ene-1-carboxylate (10)

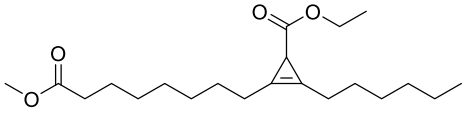

A solution of ethyl diazoacetate (15 wt. % in DCM, 0.9 mL, 1.29 mmol, 1.0 eq) was added dropwise over 3 hours to a suspension of compound **9** (333 mg, 1.25 mmol, 1.0 eq) and rhodium(II) acetate dimer (28 mg, 0.063 mmol, 0.05 eq) in DCM (0.2 M) at 0 °C under N_2 and stirred for another 30 minutes. The reaction mixture was concentrated under reduced pressure and the crude product was purified by silica gel column chromatography (Et_2O / pentane 1:49 to 1:9) to afford the compound **10** (327 mg, 0.928 mmol, 76% yield) as a light yellow oil. **^{1}H NMR** (400 MHz, $CDCl_3$) δ 4.06 (q, *J* = 7.1 Hz, 2H), 3.62 (s, 3H), 2.35 (t, *J* = 7.3 Hz, 4H), 2.26 (t, *J* = 7.5 Hz, 2H), 1.98 (s, 1H), 1.62 – 1.55 (m, 2H), 1.55 – 1.45 (s, 4 Hz), 1.35 – 1.16 (m, 12H), 1.20 (t, *J* = 7.2 Hz, 3H), 0.85 (t, *J* = 6.8 Hz, 3H). **^{13}C NMR** (101 MHz, $CDCl_3$) δ 177.1, 174.3, 105.8, 105.6, 59.8, 51.5, 34.1, 31.6 29.1, 29.1, 29.0, 29.0, 27.0, 27.0, 25.0, 24.6, 24.5, 22.6, 22.3, 14.5, 14.1.

2-(7-carboxyheptyl)-3-hexylcycloprop-2-ene-1-carboxylic acid (11)

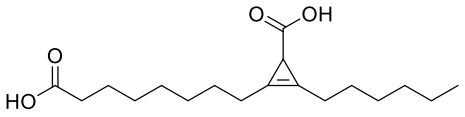

An aqueous solution of KOH (2.0 M, 4.2 mmol, 2.1 mL, 5.0 eq) was added to a solution of compound **10** (296 mg, 0.840 mmol, 1.0 eq) in ethanol (0.2 M) and refluxed for 2.5 h. The reaction mixture was acidified with aq. 1 M HCl and extracted with Et_2O (5x). The combined organic layers were washed with brine, dried over $MgSO_4$ and concentrated under reduced pressure. The crude product was purified by silica

gel column chromatography (Et_2O / pentane 1:3 + 1% AcOH) to afford the compound **11** (254 mg, 0.819 mmol, 97% yield) as a clear oil. **^{1}H NMR** (400 MHz, $CDCl_3$) δ 11.07 (s, 2H), 2.38 (t, *J* = 7.2 Hz, 4H), 2.30 (t, *J* = 7.5 Hz, 2H), 1.99 (s, 1H), 1.64 – 1.46 (m, 6H), 1.38 – 1.18 (m, 12H), 0.85 (t, *J* = 6.7 Hz, 3H).

8-(2-hexylcycloprop-1-en-1-yl)octanoic acid (3)

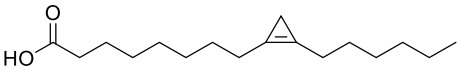

In a slightly modified procedure from the literature,[54] thionylchloride (0.48 mL, 6.62 mmol, 8.1 eq) was added to a solution of compound **11** (254 mg, 0.819 mmol, 1.0 eq) in anhydrous Et_2O (0.2 M) under N_2 atmosphere at 0 °C and stirred for 1 h. The reaction mixture was concentrated under reduced pressure and a solution of the crude acid chloride in anhydrous DCM (0.2 M) was added to anhydrous $ZnCl_2$ (221 mg, 1.622 mmol, 2.0 eq) under N_2 atmosphere. The suspension was stirred for 1 h and periodically flushed with N_2 gas, after which additional anhydrous $ZnCl_2$ (271 mg, 1.988 mmol, 2.4 eq) was added and stirred for another 2 hours. Then, methanol (0.035 mL, 0.87 mmol, 1.06 eq) was added dropwise and stirred for 30 min. The reaction mixture was added to a solution of $NaBH_4$ (167 mg, 4.41 mmol, 5.4 eq) and NaOH (74 mg, 1.85 mmol, 2.25 eq) in anhydrous meOH (0.1 M) at -30 °C and stirred for 1 h gradually warming to rt. The reaction was quenched with water, acidified with aq. 1 M HCl and extracted with DCM (3x). The combined organic layers were washed with water, sat. aq. $NaHCO_3$ and brine, dried over $MgSO_4$ and concentrated under reduced pressure. The crude product was purified by silica gel column chromatography (Et_2O / pentane 1:9) to afford compound **3** (21 mg, 0.079 mmol, 10% yield). **^{1}H NMR** (400 MHz, $CDCl_3$) δ 2.37 (t, *J* = 7.2Hz, 4H), 2.35 (t, *J* = 7.68Hz, 2H), 1.71 – 1.58 (m, 2H), 1.59 – 1.46 (m, 4H), 1.42 – 1.15 (m, 12H), 0.88 (t, *J* = 6.8 Hz, 3H), 0.76 (s, 2H). **^{13}C NMR** (101 MHz, $CDCl_3$) δ 179.7, 109.5, 109.2, 34.0, 31.7, 29.2, 29.1, 29.0, 29.0, 27.4, 27.3, 26.1, 26.0, 24.7, 22.6, 14.1, 7.4.

1,1,2-tribromo-2-methylcyclopropane (14)

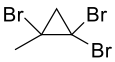

General procedure C was used with 2-bromoprop-1-ene **12** (4.50 g, 37.20 mmol, 1.0 eq) as starting material to afford the title compound **4** (5.10 g, 17.42 mmol, 47% yield) as a colorless liquid. **^{1}H NMR** (300 MHz, $CDCl_3$) δ 2.08 (s, 3H), 1.98 (d, *J* = 9.2 Hz, 1H), 1.84 (d, *J* = 9.2 Hz, 1H). **^{13}C NMR** (75 MHz, $CDCl_3$) δ 39.7, 38.6, 33.3, 30.0. Spectral data was in accordance with the literature.[79]

1-(12-iodododecyl)-2-methylcycloprop-1-ene (16)

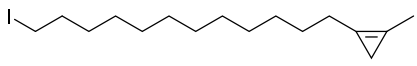

General procedure D was used with compound **14** (410 mg, 1.40 mmol, 1.0 eq) and 1,12-diiododododecane (1.48 g, 3.50 mmol, 2.5 eq) as starting materials to afford the title compound **16** (134 mg, 0.38 mmol, 27 % yield). **^{1}H NMR** (300 MHz, $CDCl_3$) δ 3.18 (t, *J* = 7.1 Hz, 2H), 2.36 (tq, *J* = 7.3, 1.7 Hz, 2H), 2.03 (t, *J* = 1.6 Hz, 3H), 1.82 (p, *J* = 7.1 Hz, 2H), 1.58 – 1.48 (m, 2H), 1.43 – 1.24 (m, 16H), 0.77 (s, 2H). **^{13}C NMR** (75 MHz, $CDCl_3$) δ 110.2, 105.3, 33.7, 30.7, 29.7, 29.7, 29.6, 29.5, 28.7, 27.5, 26.1, 11.7, 8.3, 7.5.

13-(2-methylcycloprop-1-en-1-yl)tridecanenitrile (19)

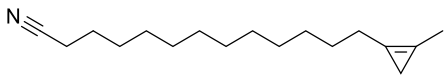

General procedure E was used with compound **16** (134 mg, 0.38 mmol, 1.0 eq) as starting material to afford the title compound **19** (76 mg, 0.31 mmol, 80 % yield). **^{1}H NMR** (300 MHz, $CDCl_3$) δ 2.40 – 2.32 (m, 2H), 2.33 (t, *J* = 7.1 Hz, 2H), 2.03 (t, *J* = 1.6 Hz, 3H), 1.73 – 1.57 (m, 2H), 1.59 – 1.38 (m, 4H), 1.37 – 1.18 (m, 14H), 0.77 (s, 2H). **^{13}C NMR** (75 MHz, $CDCl_3$) δ 120.0, 110.2, 105.3, 29.7, 29.6, 29.5, 29.5, 29.4, 28.9, 28.8, 27.5, 26.1, 25.5, 17.3, 11.7, 8.2.

13-(2-methylcycloprop-1-en-1-yl)tridecanoic acid (1)

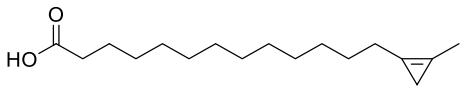

General procedure F was used with compound **19** (76 mg, 0.31 mmol, 1.0 eq) as starting material to afford the title compound **1** (30 mg, 0.11 mmol, 37% yield). **^{1}H NMR** (300 MHz, $CDCl_3$) δ 2.41 – 2.29 (m, 4H), 2.03 (t, *J* = 1.5 Hz 3H), 1.63 (p, *J* = 7.4 Hz, 2H), 1.59 – 1.46 (m, 2H), 1.38 – 1.16 (m, 16H), 0.77 (s, 2H). ^{13}C NMR (75 MHz, $CDCl_3$) δ 179.8, 110.1, 105.2, 34.0, 29.6, 29.6, 29.6, 29.4 29.4, 29.4, 29.3, 29.1, 27.4, 26.0, 24.7, 11.5, 8.1.

1-(14-iodotetradecyl)-2-methylcycloprop-1-ene (17)

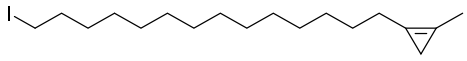

General procedure D was used with compound **14** (488 mg, 1.67 mmol, 1.0 eq) and 1,14-diiodotetradecane (1.58 g, 3.34 mmol, 2.2 eq) as starting materials to afford the title compound **17** (280 mg, 0.74 mmol, 45% yield). **^{1}H NMR** (300 MHz, $CDCl_3$) δ 3.18 (t, *J* = 7.1 Hz, 2H), 2.48 – 2.28 (m, 2H), 2.03 (t, *J* = 1.6 Hz, 3H), 1.82 (p, *J* = 7.1 Hz, 2H), 1.60 – 1.47 (m, 2H), 1.43 – 1.17 (m, 20H),

0.77 (s, 2H). **^{13}C NMR** (75 MHz, $CDCl_3$) δ 110.2, 105.3, 33.7, 30.7, 29.8, 29.8, 29.7, 29.6, 29.5, 28.7, 27.5, 26.1, 11.7, 8.3, 7.3.

15-(2-methylcycloprop-1-en-1-yl)pentadecanenitrile (20)

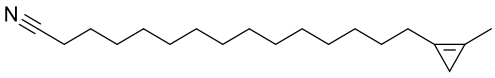

General procedure E was used with compound **17** (280 mg, 0.74 mmol, 1.0 eq) as starting material to afford the title compound **20** (140 mg, 0.51 mmol, 68 % yield). **^{1}H NMR** (300 MHz, $CDCl_3$) δ 2.49 – 2.28 (m, 4H), 2.03 (t, *J* = 1.6 Hz 3H), 1.75 – 1.40 (m, 6H), 1.39 – 1.18 (m, 18H), 0.79 (s, 2H). **^{13}C NMR** (75 MHz, $CDCl_3$) δ 120.0, 110.2, 105.3, 29.8, 29.7, 29.6, 29.6, 29.5, 29.4, 28.9, 28.8, 27.5, 26.1, 25.5, 17.3, 11.7, 8.2.

15-(2-methylcycloprop-1-en-1-yl)pentadecanoic acid (2)

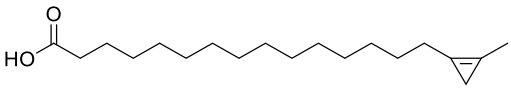

General procedure F was used with compound **20** (140 mg, 0.51 mmol, 1.0 eq) as starting material to afford the title compound **2** (89 mg, 0.30 mmol, 60% yield). **^{1}H NMR** (300 MHz, $CDCl_3$) δ 10.38 (br s, 1H), 2.43 – 2.29 (m, 4H), 2.03 (t, *J* = 1.6 Hz, 3H), 1.63 (p, *J* = 7.4 Hz, 2H), 1.59 – 1.46 (m, 2H), 1.38 – 1.17 (m, 20H), 0.77 (s, 2H). **^{13}C NMR** (75 MHz, $CDCl_3$) δ 180.6, 110.2, 105.3, 34.3, 29.8, 29.8, 29.8, 29.8, 29.7, 29.6, 29.6, 29.6, 29.4, 29.2, 27.5, 26.1, 24.8, 11.7, 8.3.

2-bromodec-1-ene (13)

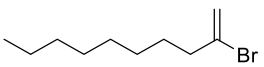

General procedure B was used with dec-1-yne (0.90 mL, 5.0 mmol, 1.0 eq) as starting material to afford the title compound **13** (854 mg, 3.90 mmol, 78% yield) as a colorless liquid. **^{1}H NMR** (400 MHz, $CDCl_3$): δ 5.55 (dt, *J* = 1.6 Hz, 1.2 Hz, 1H), 5.38 (d, *J* = 1.6 Hz, 1H), 2.49 – 2.34 (dt, *J* = 2.8, 1.2, 3H), 1.65 – 1.49 (m, 3H), 0.95 – 0.82 (t, *J* = 7.0 Hz, 3H). **^{13}C NMR** (101 MHz, $CDCl_3$): δ 135.1, 116.3, 41.6, 32.0, 29.4, 29.4, 28.6, 28.1, 22.8, 14.3. Spectral data was in accordance with the literature.[79]

1,1,2-tribromo-2-octylcyclopropane (15)

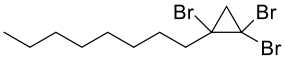

General procedure C was used with compound **13** (3.22 g, 14.7 mmol, 1.0 eq) as starting material to afford the title compound **15** (2.69 g, 6.88 mmol, 47% yield) as a colorless liquid. **^{1}H NMR** (400 MHz, $CDCl_3$): δ 2.11-1.93 (m, 2H) 1.97 – 1.93 (d, *J* = 9.2 Hz

1H), 1.82 (d, *J* = 9.2 Hz, 1H), 1.79 – 1.53 (m, 1H), 1.43 – 1.16 (m, 14H), 0.95 – 0.85 (t, *J* = 7.0 Hz , 3H). **^{13}C NMR** (101 MHz, $CDCl_3$): δ 46.0, 41.9, 38.2, 33.3, 32.0, 29.6, 29.4, 29.1, 27.8, 22.8, 14.3. Spectral data was in accordance with the literature.[75]

1-(7-iodoheptyl)-2-octylcycloprop-1-ene (18)

General procedure D was used with compound **15** (3.91 g, 10.0 mmol, 1.0 eq) and 1,7-diiodoheptane (8.10 g, 23.0 mmol, 2.3 eq) as starting materials to afford the title compound **18** (2.10 g, 5.59 mmol, 56 % yield). **^{1}H NMR** (400 MHz, $CDCl_3$): δ 3.18 (t, *J* = 7.0 Hz, 2H), 2.41 – 2.33 (m, 4H), 1.82 (p, *J* = 7.1 Hz, 2H), 0.92-0.85 (m, 3H), 0.77 (s, 2H).). **^{13}C NMR** (101 MHz, $CDCl_3$): δ 109.6, 109.3, 33.7, 32.0, 30.6, 29.6, 29.4, 29.3, 28.5, 27.5, 27.4, 26.2, 26.1, 22.8, 14.3, 7.5, 7.3.

8-(2-octylcycloprop-1-en-1-yl)octanenitrile (21)

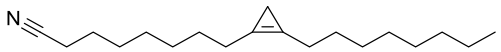

General procedure E was used with compound **18** (2.10 g, 5.59 mmol, 1.0 eq) as starting material to afford the title compound **21** (1.39 g, 5.00 mmol, 89 % yield) as a clear oil. **^{1}H NMR** (300 MHz, $CDCl_3$): δ 0.92 – 0.85 (m, 3H), 0.76 (s, 2H). **^{13}C NMR** (75 MHz, $CDCl_3$): δ 119.9, 109.7, 109.2, 32.0, 29.5, 29.4, 29.2, 28.8, 28.7, 27.5, 27.4, 26.2, 26.0, 25.5, 22.8, 17.3, 14.3, 7.5.

8-(2-octylcycloprop-1-en-1-yl)octanoic acid (4)

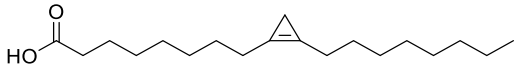

General procedure F was used with compound **21** (1.35 g, 4.92 mmol, 1.0 eq) as starting material to afford the title compound **4** (909 mg, 3.09 mmol, 63% yield) as a light yellow oil. **^{1}H NMR** (300 MHz, $CDCl_3$): δ 2.24-2.28 (m, 6H) 0.93 – 0.83 (m, 3H), 0.77 (s, 2H). **^{13}C NMR** (75 MHz, $CDCl_3$): δ 180.3, 109.6, 109.4, 34.2, 32.0, 29.6, 29.4, 29.3, 29.2, 27.5, 27.5, 26.2, 26.1, 24.8, 22.8, 14.3, 7.5.

2-bromohept-1-ene (26)

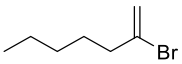

General procedure B was used with hept-1-yne (7.33 g, 76.22 mmol, 1.0 eq) as starting material to afford the title compound **26** (7.05 g, 39.81 mmol, 52% yield) as a colorless liquid. ^{1}H NMR (400 MHz, $CDCl_3$) δ 5.55 (dt, *J* = 1.6, 1.2 Hz, 1H), 5.38 (d, *J* = 1.6 Hz, 1H), 2.41 (td, *J* = 7.4, 1.2 Hz, 2H), 1.65 – 1.48 (m, 2H), 1.39 – 1.15 (m, 4H), 0.90 (t, *J* = 7.0 Hz, 3H). Spectral data was in accordance with the literature.[80]

1,1,2-tribromo-2-pentylcyclopropane (27)

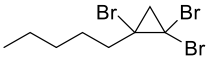

General procedure C was used with compound **26** (7.05 g, 39.81 mmol, 1.0 eq) as starting material to afford the title compound **27** (7.88 g, 22.57 mmol, 57% yield) as a colorless liquid. ^{1}H NMR (400 MHz, $CDCl_3$) δ 2.13 – 1.99 (m, 2H), 1.98 (dd, *J* = 9.1, 0.8 Hz, 1H), 1.85 (d, *J* = 9.2 Hz, 1H), 1.82 – 1.58 (m, 2H), 1.48 – 1.29 (m, 4H), 1.10 – 0.84 (m, 3H). Spectral data was in accordance with the literature.[81]

2-(2-pentylcycloprop-1-en-1-yl)ethan-1-ol (28)

A solution of *n*-Buli (1.6 M in hexanes, 7.80 mL, 12.48 mmol, 2.2 eq) was added dropwise to a solution of compound **27** (1.98 g, 5.67 mmol, 1 eq) at -78 °C under N_2 atmosphere and stirred for 30 min. A solution of oxirane (2.5 – 3.3 M in THF, 4.54 mL, 11.35 mmol, 2 eq) and BF3·OEt (7.8 ml, 12.48 mmol, 2.2 eq) were added carefully and the reaction mixture was stirred for 15 min at -78 °C and for 1 h at 0 °C. The reaction was quenched with sat. aq. NH_4Cl and extracted with Et_2O (3x). The combined organic layers were washed with brine, dried over $MgSO_4$ and concentrated under reduced pressure. The crude product was purified by silica gel column chromatography (Et_2O / pentane 1:9 to 1:4) to afford compound **28** (428 mg, 2.77 mmol, 49% yield) as a light yellow oil. **^{1}H NMR** (400 MHz, $CDCl_3$) δ 3.84 (t, *J* = 6.3 Hz, 2H), 2.68 (tt, *J* = 6.2, 1.6 Hz, 2H), 2.41 (tt, *J* = 7.3, 1.6 Hz, 2H), 1.61 – 1.52 (m, 2H), 1.50 (br s, 1H), 1.41 – 1.23 (m, 4H), 0.95 – 0.86 (m, 3H), 0.84 (s, 2H).

1-(2-bromoethyl)-2-pentylcycloprop-1-ene (29)

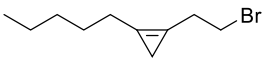

N-bromosuccinimide (506 mg, 3.28 mmol, 1 eq) and triphenylphosphine (1.03 mg, 3.94 mmol, 1.2 eq) were added in one portion to a solution of compound **28** (700 mg, 3.94 mmol, 1.2 eq) in anh. DCM at 0 °C under N_2 atmosphere and stirred at rt for 1 h. The

reaction mixture was quenched with sat. aq. $NaHCO_3$ and extracted with DCM (3x). The combined organic layers were washed with brine, dried over $MgSO_4$ and concentrated under reduced pressure. The crude product was purified by silica gel column chromatography (pentane) to afford compound **29** (417 mg, 1.92 mmol, 59% yield) as a light yellow oil. **^{1}H NMR** (400 MHz, $CDCl_3$) δ 3.54 (t, *J* = 7.0 Hz, 2H), 2.99 (tt, *J* = 7.1, 1.6 Hz, 2H), 2.42 (tt, *J* = 7.3, 1.5 Hz, 2H), 1.62 – 1.51 (m, 2H), 1.39 – 1.21 (m, 4H), 0.93 – 0.87 (m, 3H), 0.86 (s, 2H). **^{13}C NMR** (101 MHz, $CDCl_3$) δ 112.9, 106.7, 31.7, 30.2, 30.2, 27.0, 26.2, 22.6, 14.2, 7.6.

(2-(2-pentylcycloprop-1-en-1-yl)ethyl)triphenylphosphonium bromide (24)

General procedure G was used with compound **29** (49 mg, 0.23 mmol, 1.0 eq) as starting material to afford the title compound **24** (89 mg, 0.19 mmol, 82% yield) as a light yellow oil. **^{1}H NMR** (400 MHz, $CDCl_3$) δ 7.99 – 7.64 (m, 15H), 3.96 (dt, *J* = 12.1, 7.0 Hz, 2H), 3.00 (dtt, *J* = 17.4, 7.1, 1.5 Hz, 2H), 2.23 (tt, *J* = 7.3, 1.6 Hz, 2H), 1.47 – 1.35 (m, 2H), 1.35 – 1.14 (m, 4H), 0.85 (t, *J* = 7.0 Hz, 3H), 0.60 (s, 2H). **^{13}C NMR (**101 MHz, $CDCl_3$) δ 135.3, 135.2, 133.6, 133.5, 130.6, 130.5, 118.2, 117.3, 113.5, 105.7, 105.6, 31.4, 26.7, 25.5, 22.3, 21.5, 21.0, 19.5, 19.5, 14.0, 7.9.

9-((tert-butyldimethylsilyl)oxy)nonan-1-ol (30)

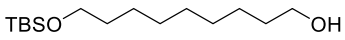

Imidazole (510 mg, 7.49 mmol, 1.2 eq) and TBSCl (940 mg, 6.24 mmol, 1 eq) were added to a solution of nonane-1,9-diol (2.0 g, 12.48 mmol, 2 eq) in anh. DCM at rt under N_2 atmosphere and stirred for 3 h. The reaction mixture was diluted with water and extracted with DCM (3x). The combined organic layers were washed with brine, dried over $MgSO_4$ and concentrated under reduced pressure. The crude product was purified by silica gel column chromatography (Et_2O / pentane 1:4 to 1:2) to afford compound **30** (1.10 g, 4.0 mmol, 64% yield) as a clear oil. **^{1}H NMR** (400 MHz, $CDCl_3$) δ 3.64 (td, *J* = 6.7, 5.2 Hz, 2H), 3.59 (t, *J* = 6.6 Hz, 2H), 1.64 – 1.44 (m, 4H), 1.40 – 1.27 (m, 10H), 0.89 (s, 9H), 0.04 (s, 6H). ^{1}H NMR (400 MHz, $CDCl_3$) δ 3.63 (t, *J* = 6.6 Hz, 2H), 3.59 (t, *J* = 6.6 Hz, 2H), 1.61 – 1.44 (m, 4H), 1.37 – 1.22 (m, 10H), 0.89 (s, 9H), 0.04 (s, 6H). **^{13}C NMR** (101 MHz, $CDCl_3$) δ 63.5, 63.2, 33.0, 32.9, 29.7, 29.5, 26.1, 25.9, 25.9, 18.5, -5.1. Spectral data was in accordance with the literature.[82]

9-((tert-butyldimethylsilyl)oxy)nonanoic acid (31)

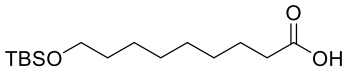

General procedure A was used with compound **30** (1.16 g, 4.02 mmol, 1.0 eq) as starting material, the crude product was purified by silica gel column chromatography (Et_2O / pentane 1:4, 1% AcOH) to afford compound **31** (1.07 g, 3.70 mmol, 92% yield) as a light yellow oil. **^{1}H NMR** (400 MHz, $CDCl_3$) δ 3.59 (t, *J* = 6.6 Hz, 2H), 2.34 (t, *J* = 7.5 Hz, 2H), 1.63 (p, *J* = 7.5 Hz, 2H), 1.54 – 1.45 (m, 2H), 1.38 – 1.24 (m, 8H), 0.89 (s, 9H), 0.04 (s, 6H). **^{13}C NMR** (101 MHz, $CDCl_3$) δ 180.3, 63.4, 34.2, 33.0, 29.4, 29.1, 26.1, 25.9, 24.8, 18.5, -5.1. Spectral data was in accordance with the literature.[82]

methyl 9-((tert-butyldimethylsilyl)oxy)nonanoate (32)

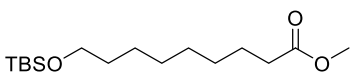

Methyl iodide (0.43 mL, 6.93 mmol, 2 eq) and K_2CO_3 (1.44 g, 10.4 mmol, 3 eq) were added to a solution of compound **31** (1.0 g, 3.47 mmol, 1 eq) in anh. DMF at rt under N_2 atmosphere and stirred for 18 h. The reaction mixture was diluted (10x) with sat. aq. $NaHCO_3$ and extracted with Et_2O (3x). The combined organic layers were washed with brine, dried over $MgSO_4$ and solvents removed under reduced pressure. The crude product was purified by silica gel column chromatography (Et_2O / pentane 1:9) to afford compound **32** (898 mg, 2.97 mmol, 86% yield). **^{1}H NMR** (400 MHz, $CDCl_3$) δ 3.66 (s, 3H), 3.59 (t, *J* = 6.6 Hz, 2H), 2.30 (t, *J* = 7.6 Hz, 2H), 1.70 – 1.56 (m, 2H), 1.55 – 1.43 (m, 2H), 1.35 – 1.23 (m, 8H), 0.89 (s, 9H), 0.04 (s, 6H). **^{13}C NMR** (101 MHz, $CDCl_3$) δ 174.5, 63.4, 51.6, 34.2, 33.0, 29.4, 29.2, 26.1, 25.9, 25.1, 18.5, -5.1. Spectral data was in accordance with the literature.[83]

methyl 9-hydroxynonanoate (33)

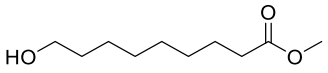

A solution of TBAF (1.0 M in THF, 8.73 mL, 8.73 mmol, 3 eq) was added dropwise to a solution of compound **32** (880 mg, 2.91 mmol, 1 eq) in anh. THF (0.3 M) at 0 °C under N_2 atmosphere and stirred for 5 h at rt. The reaction mixture was diluted with aq. 1 M HCl and extracted with DCM (3x). The combined organic layers were washed with brine, dried over $MgSO_4$ and solvents removed under reduced pressure. The crude product was purified by silica gel column chromatography (EtOAc/pentane 1:4 to 1:1) to afford compound **33** (512 mg, 2.72 mmol, 93% yield) **^{1}H NMR** (400 MHz, $CDCl_3$) δ 3.65 (s, 3H), 3.61 (t, *J* = 6.6 Hz, 2H), 2.28 (t, *J* = 7.5 Hz, 2H), 1.68 – 1.47 (m, 4H), 1.38 – 1.23 (m, 8H). **^{13}C NMR** (101 MHz,

$CDCl_3$) δ 174.5, 63.1, 51.6, 34.2, 32.8, 29.3, 29.1, 25.8, 25.0. Spectral data was in accordance with the literature. [84]

methyl 9-oxononanoate (25)

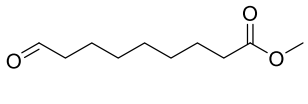

Dess-Martin periodinane (1.41 g, 3.32 mmol, 1.3 eq) was added to a solution of compound **33** (481 mg, 2.55 mmol, 1 eq) in anh. DCM (0.2 M) at 0 °C under N_2 atmosphere and stirred for 1 h at rt. The reaction mixture was quenched with sat. aq. $NaHCO_3$ and extracted with Et_2O (3x). The combined organic layers were washed with brine, dried over $MgSO_4$ and solvents removed under reduced pressure. The crude product was purified by silica gel column chromatography (Et_2O / pentane 1:4) to afford compound **25** (372 mg, 2.0 mmol, 78% yield) as a light yellow oil. **^{1}H NMR** (400 MHz, $CDCl_3$) δ 9.75 (t, *J* = 1.6, 1H), 3.65 (s, 3H), 2.41 (td, *J* = 7.3, 1.8 Hz, 2H), 2.29 (t, *J* = 7.5 Hz, 2H), 1.70 – 1.52 (m, 4H), 1.39 – 1.22 (m, 6H). **^{13}C NMR** (101 MHz, $CDCl_3$) δ 202.9, 174.3, 51.6, 43.9, 34.1, 29.1, 29.0, 29.0, 24.9, 22.1. Spectral data was in accordance with the literature. [84]

methyl (Z)-11-(2-pentylcycloprop-1-en-1-yl)undec-9-enoate (34)

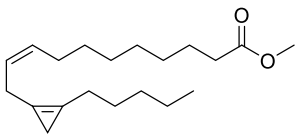

A solution of NaHMDS (1 M, 0.27 mL, 0.27 mmol, 1 eq) was added dropwise to a solution of compound **24** (128 mg, 0.12 mmol, 1 eq) in anh. THF (0.25 M) at -78 °C under N_2 atmopshere and stirred for 1 h. A solution of compound **25** (60 mg, 0.32 mmol, 1.2 eq) in anh. THF (0.5 M) was added dropwise to the orange brown suspension and stirred for 1.5 h. The reaction mixture was quenched with sat. aq. NH_4Cl and extracted with Et_2O (3x). The combined organic layers were washed with brine, dried over $MgSO_4$ and solvents removed under reduced pressure. The crude product was purified by silica gel column chromatography (Et_2O / pentane 1:99 to 1:49) to afford compound **34** (36 mg, 0.12 mmol, 44% yield) as a clear colorless oil. **^{1}H NMR** (500 MHz, $CDCl_3$) δ 5.55 – 5.41 (m, 2H), 3.66 (s, 3H), 3.12 (d, *J* = 6.3 Hz, 2H), 2.37 (tt, *J* = 7.3, 1.6 Hz, 2H), 2.29 (t, *J* = 7.6 Hz, 2H), 2.05 (q, *J* = 7.1, 6.7 Hz, 2H), 1.66 – 1.56 (m, 2H), 1.57 – 1.49 (m, 2H), 1.39 – 1.24 (m, 12H), 0.89 (t, *J* = 6.9 Hz, 3H), 0.81 (s, 2H). **^{13}C NMR** (126 MHz, $CDCl_3$) δ 174.4, 131.3, 125.3, 110.1, 108.1, 51.6, 34.2, 31.7, 29.6, 29.3, 29.2, 29.2, 27.3, 27.3, 26.1, 25.1, 24.8, 22.6, 14.2, 7.8.

(Z)-11-(2-pentylcycloprop-1-en-1-yl)undec-9-enoic acid (5)

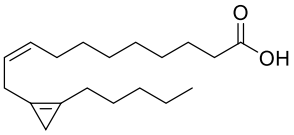

General procedure H was used with compound **34** (36 mg, 0.12 mmol, 1.0 eq) as starting material to afford the title compound **5** (25 mg, 85 µmol, 73% yield) as a light yellow oil. **^{1}H NMR** (400 MHz, $CDCl_3$) δ 11.02 (br s, 1H), 5.66 – 5.31 (m, 2H), 3.13 (d, *J* = 6.4 Hz, 2H), 2.43 – 2.29 (m, 4H), 2.12 – 2.00 (m, 2H), 1.70 – 1.49 (m, 4H), 1.43 – 1.23 (m, 12H), 0.92 – 0.87 (m, 3H), 0.81 (s, 2H). **^{13}C NMR** (101 MHz, $CDCl_3$) δ 180.4, 131.3, 125.3, 110.1, 108.1, 34.2, 31.8, 29.6, 29.3, 29.2, 29.2, 27.3, 27.3, 26.1, 24.8, 24.8, 22.6, 14.2, 7.8.

methyl 7-hydroxyhept-5-ynoate (37)

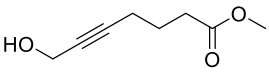

In a slightly modified procedure from the literature[85], a solution of EtMgBr (3.0 M in Et_2O, 45.5 mL, 136.5 mmol, 3 eq) was added to a solution of hex-5-ynoic acid (5.10 g, 45.5 mmol, 1 eq) in anh. THF (0.2 M) at 0 °C under N_2 atmosphere and stirred for 1 h slowly warming to rt. Then, paraformaldehyde (2.73 g, 91.0 mmol, 2 eq) was added portionwise to the grey suspension and the reaction mixture was stirred at 75 °C for 18 h. The reaction mixture was quenched with aq. 1 M HCl and extracted with DCM (3x). The combined organic layers were washed with brine, dried over $MgSO_4$ and solvents removed under reduced pressure. Thionyl chloride (6.60 mL, 91.0 mmol, 2 eq) was added carefully to a solution of the crude product in anh. MeOH (0.2 M) at 0 °C under N_2 atmosphere and stirred for 1 h at rt. The reaction mixture was concentrated under reduced pressure and the crude product was purified by silica gel column chromatography (Et_2O / pentane 1:2) to afford compound **37** (3.60 g, 23.1 mmol, 51% yield) as a clear oil. **^{1}H NMR** (400 MHz, $CDCl_3$) δ 4.23 (t, *J* = 2.2 Hz, 2H), 3.67 (s, 3H), 2.43 (t, *J* = 7.4 Hz, 2H), 2.28 (tt, *J* = 6.9, 2.2 Hz, 2H), 1.82 (p, *J* = 7.1 Hz, 2H). **^{13}C NMR** (101 MHz, $CDCl_3$) δ 173.8, 85.1, 79.4, 51.8, 51.4, 32.9, 23.8, 18.3. Spectral data was in accordance with the literature.[86]

methyl 7-bromohept-5-ynoate (38)

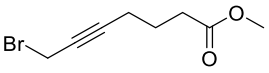

N-bromosuccinimide (1.16 g, 6.53 mmol, 1.2 eq) and triphenylphosphine (1.71 g, 6.53 mmol, 1.2 eq) were added to a solution of compound **37** (855 mg, 5.44 mmol, 1 eq) in anh. DCM (0.2 M) at 0 °C under N_2 atmosphere and stirred for 1 h at rt. The reaction mixture was quenched with sat. aq. $NaHCO_3$ and extracted

with DCM (3x). The combined organic layers were washed with brine, dried over $MgSO_4$ and solvents removed under reduced pressure. The crude product was purified by silica gel column chromatography (Et_2O / pentane 1:19) to afford compound **38** (980 mg, 4.47 mmol, 82% yield) as a light yellow oil. **^{1}H NMR** (400 MHz, $CDCl_3$) δ 3.90 (t, *J* = 2.4 Hz, 2H), 3.67 (s, 3H), 2.42 (t, *J* = 7.4 Hz, 2H), 2.31 (tt, *J* = 6.9, 2.4 Hz, 2H), 1.82 (p, *J* = 7.1 Hz, 2H). **^{13}C NMR** (101 MHz, $CDCl_3$) δ 173.6, 86.8, 76.3, 51.7, 32.8, 23.6, 18.5, 15.5. Spectral data was in accordance with the literature.[86]

methyl 11-hydroxyundeca-5,8-diynoate (36)

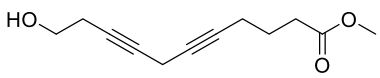

Copper(I)iodide (447 mg, 2.92 mmol, 2 eq), Sodium iodide (438 mg, 2.92 mmol, 2 eq) and K_2CO_3 (404 mg, 2.92 mmol, 2 eq) were added to a solution of but-3-yn-1-ol (0.22 mL, 2.92 mmol, 2 eq) in anh. DMF (0.2 M) at rt under N_2 atmosphere and stirred for 30 min at rt. Then, a solution of compound **38** (320 mg, 1.46 mmol, 1 eq) in anh. DMF (1.0 M) was added dropwise to the reaction mixture and stirred for 18 h. The suspension was diluted with sat. aq. NH_4Cl and extracted with Et_2O (3x). The combined organic layers were washed with sat. aq. $Na_2S_2O_3$ and brine, dried over $MgSO_4$ and solvents removed under reduced pressure. The crude product was purified by silica gel column chromatography (Et_2O / pentane 1:1) to afford compound **36** (220 mg, 1.06 mmol, 72% yield) as a light yellow oil. **^{1}H NMR** (400 MHz, $CDCl_3$) δ 3.67 (t, *J* = 6.3 Hz, 2H), 3.65 (s, 3H), 3.10 (p, *J* = 2.4 Hz, 2H), 2.46 – 2.36 (m, 4H), 2.21 (tt, *J* = 6.9, 2.4 Hz, 2H), 2.17 – 2.04 (m, 1H), 1.79 (p, *J* = 7.1 Hz, 2H). **^{13}C NMR** (101 MHz, $CDCl_3$) δ 173.8, 79.5, 77.1, 76.6, 75.2, 61.2, 51.7, 33.0, 23.9, 23.2, 18.3, 9.8. Spectral data was in accordance with the literature.[86]

methyl (5Z,8Z)-11-hydroxyundeca-5,8-dienoate (39)

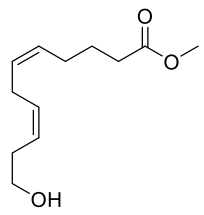

In a slightly modified procedure from the literature,[64] a solution of $NaBH_4$ (111 mg, 2.94 mmol, 2 eq) in degassed anh. MeOH (1.5 M) was added to a solution of Nickel(II) acetate hydrate (658 mg, 2.64 mmol, 1.8 eq) in MeOH (1.5 M) at rt under N_2 atmosphere, the solution turned dark black immediately and was purged with H_2 for 5 min. Ethylenediamine (0.18 ml, 2.64 mmol, 1.8 eq) and a solution of compound **36** (306 mg, 1.47 mmol, 1 eq) in MeOH (1.5 M) were added and the reaction mixture was stirred under positive H_2 pressure for 2 h at rt and monitored using LCMS. The suspension was diluted with Et_2O, filtered over celite, washed

with brine and dried over $MgSO_4$. The crude product was purified by silica gel column chromatography (Et2O / pentane 1:1) to afford a mixture of under / over reduced or even cis / trans products (200 mg, 0.94 mmol, 64 % yield). This was purified by HPLC (Solvent system: A: water (gradient, 10-90%), B: CH_3CN (gradient, 90-10%), C: (constant, 10%) 1% TFA (aq.) to afford compound **39** (84 mg, 0.40 mmol, 27% yield) as a clear colorless oil. **^{1}H NMR** (400 MHz, $CDCl_3$) δ 5.52 – 5.25 (m, 4H), 3.62 (s, 3H), 3.59 (t, *J* = 6.6 Hz, 2H), 2.81 – 2.72 (m, 2H), 2.36 – 2.24 (m, 4H), 2.13 (s, 1H), 2.10 – 2.01 (m, 2H), 1.65 (p, *J* = 7.5 Hz, 2H). **^{13}C NMR** (101 MHz, $CDCl_3$) δ 174.3, 130.8, 129.0, 128.8, 125.7, 62.2, 51.6, 33.4, 30.9, 26.6, 25.8, 24.7. Spectral data was in accordance with the literature.[87]

methyl (5Z,8Z)-11-oxoundeca-5,8-dienoate (35)

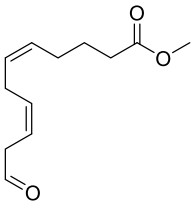

Dess-Martin periodinane (201 mg, 0.47 mmol, 1.2 eq) was added to a solution of compound **39** (84 mg, mmol, 1 eq) in anh. DCM (0.2 M) at 0 °C under N_2 atmosphere and stirred for 1 h at rt. The reaction mixture was quenched with sat. aq. $NaHCO_3$ and extracted with Et_2O (3x). The combined organic layers were washed with brine, dried over $MgSO_4$ and solvents removed under reduced pressure. The crude product was purified by silica gel column chromatography (Et_2O / pentane 1:2) to afford compound **35** (31 mg, 0.15 mmol, 37% yield) as a clear oil. **^{1}H NMR** (400 MHz, $CDCl_3$) δ 9.66 (t, *J* = 1.9 Hz, 1H), 5.72 – 5.49 (m, 2H), 5.46 – 5.30 (m, 2H), 3.65 (s, 3H), 3.26 – 3.16 (m, 2H), 2.80 – 2.73 (m, 2H), 2.30 (t, *J* = 7.4 Hz, 2H), 2.13 – 2.03 (m, 2H), 1.74 – 1.62 (m, 2H). **^{13}C NMR** (101 MHz, $CDCl_3$) δ 199.5, 174.1, 133.3, 129.7, 127.9, 118.7, 51.6, 42.6, 33.5, 26.7, 26.0, 24.8. Spectral data was in accordance with the literature.[88]

methyl (5Z,8Z,11Z)-13-(2-pentylcycloprop-1-en-1-yl)trideca-5,8,11-trienoate (40)

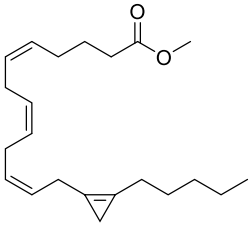

A solution of NaHMDS (1 M, 0.29 mL, 0.29 mmol, 2 eq) was added dropwise to a solution of compound **24** (140 mg, 0.29 mmol, 2 eq) in anh. THF (0.25 M) at -78 °C under N_2 atmopshere and stirred for 1 h. A solution of compound **35** (31 mg, 0.15 mmol, 1 eq) in anh. THF (0.5 M) was added dropwise to the orange brown suspension and stirred for 1.5 h. The reaction mixture was quenched with sat. aq. NH_4Cl and extracted with Et_2O (3x). The combined organic layers were washed with brine, dried over $MgSO_4$ and solvents

removed under reduced pressure. The crude product was purified by silica gel column chromatography (Et_2O / pentane 1:99 to 1:49) to afford compound **40** (26 mg, 78 µmol, 54% yield) as a clear colorless oil. **^{1}H NMR** (500 MHz, $CDCl_3$) δ 5.60 – 5.40 (m, 2H), 5.42 – 5.29 (m, 4H), 3.66 (s, 3H), 3.17 (d, *J* = 7.0 Hz, 2H), 2.85 (t, *J* = 6.5 Hz, 2H), 2.80 (t, *J* = 5.8 Hz, 2H), 2.38 (t, *J* = 7.3 Hz, 2H), 2.32 (t, *J* = 7.5 Hz, 2H), 2.11 (q, *J* = 7.0 Hz, 2H), 1.70 (p, *J* = 7.5 Hz, 2H), 1.54 (p, *J* = 7.0 Hz, 2H), 1.37 – 1.26 (m, 4H), 0.89 (t, *J* = 6.7 Hz, 3H), 0.82 (s, 2H). **^{13}C NMR** (126 MHz, $CDCl_3$) δ 174.2, 129.2, 129.1, 129.0, 128.4, 128.1, 125.8, 110.4, 107.8, 51.6, 33.6, 31.7, 27.2, 26.7, 26.0, 25.8, 25.7, 24.9, 24.8, 22.6, 14.2, 7.8.

(5Z,8Z,11Z)-13-(2-pentylcycloprop-1-en-1-yl)trideca-5,8,11-trienoic acid (6)

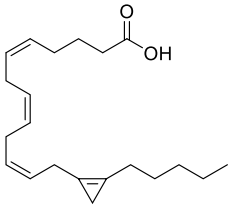

General procedure H was used with compound **40** (26 mg, 78 µmol, 1.0 eq) as starting material to afford the title compound **6** (25 mg, 78 µmol, quantitative yield) as a clear colorless oil. **^{1}H NMR** (500 MHz, $CDCl_3$) δ 11.24 (br s, 1H), 5.60 – 5.41 (m, 2H), 5.44 – 5.30 (m, 4H), 3.17 (d, *J* = 7.0 Hz, 2H), 2.85 (t, *J* = 6.6 Hz, 2H), 2.80 (t, *J* = 6.1 Hz, 2H), 2.38 (q, *J* = 8.2 Hz, 4H), 2.13 (q, *J* = 7.1 Hz, 2H), 1.72 (p, *J* = 7.5 Hz, 2H), 1.55 (p, *J* = 7.2 Hz, 2H), 1.37 – 1.25 (m, 4H), 0.89 (t, *J* = 6.5 Hz, 3H), 0.83 (s, 2H). **^{13}C NMR** (126 MHz, $CDCl_3$) δ 180.0, 129.2, 128.9, 128.4, 128.2, 125.8, 110.4, 107.9, 33.5, 31.8, 27.3, 26.6, 26.1, 25.8, 25.8, 24.8, 24.6, 22.6, 14.2, 7.9.

9-bromononanoic acid (s4)

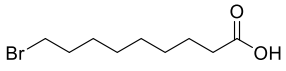

General procedure A was used with compound 9-bromononan-1-ol (3.05 g, 13.67 mmol, 1.0 eq) as starting material, the crude product was purified by silica gel column chromatography (Et_2O / pentane 1:19, 1% AcOH) to afford compound **s4** (3.09 g, 13.0 mmol, 95% yield) as a yellow oil. **^{1}H NMR** (500 MHz, $CDCl_3$) δ 11.64 (s, 1H), 3.39 (t, *J* = 6.8 Hz, 2H), 2.34 (t, *J* = 7.5 Hz, 2H), 1.89 – 1.79 (m, 2H), 1.67 – 1.58 (m, 2H), 1.46 – 1.38 (m, 2H), 1.37 – 1.27 (m, 6H).**^{13}C NMR** (126 MHz, $CDCl_3$) δ 180.6, 34.2, 34.1, 32.9, 29.1, 29.0, 28.7, 28.2, 24.7**.** Spectral data was in accordance with the literature.[89]

(8-carboxyoctyl)triphenylphosphonium bromide (s5)

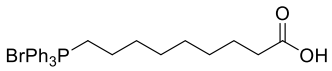

General procedure G was used with compound **s4** (3.09 g, 13.0 mmol, 1.0 eq) as starting material, the crude product was purified by silica

gel column chromatography (DCM / MeOH 99:1 to 1:19, 1% AcOH) to afford compound **s5** (6.45 g, 12.9 mmol, quant. yield) as a yellow oil. **^{1}H NMR** (500 MHz, $CDCl_3$) δ 7.80 – 7.72 (m, 9H), 7.70 – 7.65 (m, 6H), 3.62 – 3.50 (m, 2H), 2.28 (t, *J* = 7.4 Hz, 2H), 1.56 (dd, *J* = 10.4, 6.2 Hz, 4H), 1.48 (q, *J* = 7.3 Hz, 2H), 1.26 – 1.11 (m, 6H). **^{13}C NMR** (126 MHz, $CDCl_3$) δ 177.2, 135.2, 135.2, 133.7, 133.6, 130.7, 130.6, 118.6, 117. 9, 34.5, 30.2, 30.0, 28.5, 28.5, 24.6, 22.9, 22.5, 22.5. Spectral data was in accordance with the literature.[90]

(2-(1,3-dioxan-2-yl)ethyl)triphenylphosphonium bromide (s6)

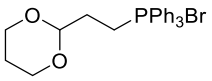

General procedure A was used with 2-(2-bromoethyl)-1,3-dioxane (1.0 mL, 7.34 mmol, 1.0 eq) as starting material to afford compound **s6** (500 mg, 1.09 mmol, 15% yield) as a yellow oil. **^{1}H NMR** (300 MHz, $CDCl_3$) δ 7.74 – 7.39 (m, 15H), 4.79 (t, *J* = 4.7 Hz, 1H), 3.83 – 3.73 (m, 2H), 3.60 (td, *J* = 12.2, 2.4 Hz, 2H), 3.54 – 3.38 (m, 2H), 1.86 – 1.74 (m, 1H), 1.73 – 1.59 (m, 2H), 1.16 – 1.05 (m, 1H). **^{13}C NMR** (75 MHz, $CDCl_3$) δ 134.8, 134.8, 133.1, 133.0, 130.3, 130.1, 118.0, 116.8, 99.0, 98.8, 66.3, 27.5, 27.5, 25.1, 17.6, 16.9.

methyl 5-oxopentanoate (s7)

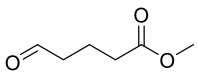

Triethylamine (22.6 mL, 122 mmol, 5 eq) was added too a solution of δ-valerolactone (3.0 mL, 32.4 mmol, 1 eq) in MeOH (0.5 M) at rt and the solution was stirred for 1 h. The solvents were removed and coevaporated with toluene to afford the crude alcohol. Dess-Martin periodinane (16.3 g, 38.4 mmol, 1.2 eq) was added to a solution of the crude alcohol (5.13 g, 38.9 mmol, 1 eq) in anh. DCM at 0 °C under N_2 atmosphere and stirred at rt for 2 h. The reaction mixture was quenched with sat. aq. $NaHCO_3$ and extracted with Et_2O (3x). The combined organic layers were washed with brine, dried over $MgSO_4$ and solvents removed under reduced pressure. The crude product was purified by silica gel column chromatography (Et_2O / pentane 1:4) to afford compound **s7** (1.96 g, 15.0 mmol, 47% yield) as a light yellow oil. **^{1}H NMR** (400 MHz, $CDCl_3$) δ 9.75 (t, *J* = 1.2 Hz, 1H), 3.65 (d, *J* = 0.9 Hz, 3H), 2.51 (tt, *J* = 7.2, 1.1 Hz, 2H), 2.36 (t, *J* = 7.3 Hz, 2H), 2.06 – 1.84 (m, 2H). **^{13}C NMR** (101 MHz, $CDCl_3$) δ 201.6, 173.5, 51.7, 43.0, 33.0, 17.4. Spectral data was in accordance with the literature.[91]

methyl (Z)-7-(1,3-dioxan-2-yl)hept-5-enoate (s8)

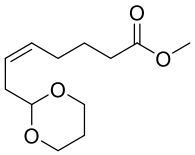

A solution of NaHMDS (1 M, 11.5 mL, 11.5 mmol, 1.3 eq) was added dropwise to a solution of compound **s6** (5.25 g, 11.5 mmol, 1.3 eq) in anh. THF (0.25 M) at -78 °C under N_2 atmopshere, slowly warmed to rt and stirred for 1 h. The reaction was cooled back to -78 °C and a solution of compound **s7** (1.15 g, 8.83 mmol, 1 eq) in anh. THF (0.5 M) was added dropwise to the orange suspension and stirred for 1.5 h. The reaction mixture was quenched with sat. aq. NH_4Cl and extracted with Et_2O (3x). The combined organic layers were washed with brine, dried over $MgSO_4$ and solvents removed under reduced pressure. The crude product was purified by silica gel column chromatography (acetone / pentane 1:49 to 1:19) to afford compound **s8** (1.31 g, 5.75 mmol, 65% yield) as a clear colorless oil. **^{1}H NMR** (300 MHz, $CDCl_3$) δ 5.58 – 5.33 (m, 2H), 4.51 (t, *J* = 5.2 Hz, 1H), 4.18 – 3.99 (m, 2H), 3.80 – 3.69 (m, 2H), 3.64 (s, 3H), 2.39 – 2.21 (m, 4H), 2.16 – 1.94 (m, 3H), 1.69 (dt, *J* = 8.3, 7.1 Hz, 2H), 1.32 (ddt, *J* = 13.5, 2.6, 1.3 Hz, 1H). **^{13}C NMR** (75 MHz, $CDCl_3$) δ 174.1, 131.3, 124.3, 101.9, 67.0, 51.5, 33.5, 26.8, 25.8, 24.8. Spectral data was in accordance with the literature.[92]

References

(1) Cucchi, D.; Camacho-Muñoz, D.; Certo, M.; Pucino, V.; Nicolaou, A.; Mauro, C. Fatty Acids - From Energy Substrates to Key Regulators of Cell Survival, Proliferation and Effector Function. *Cell Stress* **2020**, *4* (1), 9–23.

(2) De Carvalho, C. C. C. R.; Caramujo, M. J. The Various Roles of Fatty Acids. *Molecules* **2018**, *23* (10).

(3) Spector, A. A.; Yorek, M. A. Membrane Lipid Composition and Cellular Function. *J. Lipid Res.* **1985**, *26* (9), 1015–1035.

(4) Houten, S. M.; Wanders, R. J. A. A General Introduction to the Biochemistry of Mitochondrial Fatty Acid β-Oxidation. *J. Inherit. Metab. Dis.* **2010**, *33* (5), 469–477.

(5) Kimura, I.; Ichimura, A.; Ohue-Kitano, R.; Igarashi, M. Free Fatty Acid Receptors in Health and Disease. *Physiol. Rev.* **2020**, *100* (1), 171–210.

(6) Nicolaou, A.; Mauro, C.; Urquhart, P.; Marelli-Berg, F. Polyunsaturated Fatty Acid-Derived Lipid Mediators and T Cell Function. *Front. Immunol.* **2014**, *5* (FEB), 1–15.

(7) Lochner, M.; Berod, L.; Sparwasser, T. Fatty Acid Metabolism in the Regulation of T Cell Function. *Trends Immunol.* **2015**, *36* (2), 81–91.

(8) Howie, D.; Bokum, A. Ten; Necula, A. S.; Cobbold, S. P.; Waldmann, H. The Role of Lipid Metabolism in T Lymphocyte Differentiation and Survival. *Front. Immunol.* **2018**, *8* (JAN).

(9) Ikeda, T.; Nishida, A.; Yamano, M.; Kimura, I. Short-Chain Fatty Acid Receptors and Gut

Microbiota as Therapeutic Targets in Metabolic, Immune, and Neurological Diseases. *Pharmacol. Ther.* **2022**, *239*, 108273.

(10) Ichimura, A.; Hasegawa, S.; Kasubuchi, M.; Kimura, I. Free Fatty Acid Receptors as Therapeutic Targets for the Treatment of Diabetes. *Front. Pharmacol.* **2014**, *5* (NOV).

(11) Yeudall, S.; Upchurch, C. M.; Seegren, P. V.; Pavelec, C. M.; Greulich, J.; Lemke, M. C.; Harris, T. E.; Desai, B. N.; Hoehn, K. L.; Leitinger, N. Macrophage Acetyl-CoA Carboxylase Regulates Acute Inflammation through Control of Glucose and Lipid Metabolism. *Sci. Adv.* **2022**, *8* (47), 1–20.

(12) Rowland, L. A.; Guilherme, A.; Henriques, F.; DiMarzio, C.; Munroe, S.; Wetoska, N.; Kelly, M.; Reddig, K.; Hendricks, G.; Pan, M.; Han, X.; Ilkayeva, O. R.; Newgard, C. B.; Czech, M. P. De Novo Lipogenesis Fuels Adipocyte Autophagosome and Lysosome Membrane Dynamics. *Nat. Commun.* **2023**, *14* (1).

(13) Batchuluun, B.; Pinkosky, S. L.; Steinberg, G. R. Lipogenesis Inhibitors: Therapeutic Opportunities and Challenges. *Nat. Rev. Drug Discov.* **2022**, *21* (4), 283–305.

(14) Bielawiec, P.; Dziemitko, S.; Konstantynowicz-Nowicka, K.; Chabowski, A.; Dzięcioł, J.; Harasim-Symbor, E. Cannabidiol Improves Muscular Lipid Profile by Affecting the Expression of Fatty Acid Transporters and Inhibiting de Novo Lipogenesis. *Sci. Rep.* **2023**, *13* (1), 1–16.

(15) Yao, Z.; Gong, Y.; Chen, W.; Shao, S.; Song, Y.; Guo, H.; Li, Q.; Liu, S.; Wang, X.; Zhang, Z.; Wang, Q.; Xu, Y.; Wu, Y.; Wan, Q.; Zhao, X.; Xuan, Q.; Wang, D.; Lin, X.; Xu, J.; Liu, J.; Proud, C. G.; Wang, X.; Yang, R.; Fu, L.; Niu, S.; Kong, J.; Gao, L.; Bo, T.; Zhao, J. Upregulation of WDR6 Drives Hepatic de Novo Lipogenesis in Insulin Resistance in Mice. *Nat. Metab.* **2023**, *5* (October).

(16) Luukkonen, P. K.; Porthan, K.; Ahlholm, N.; Rosqvist, F.; Dufour, S.; Zhang, X. M.; Lehtimäki, T. E.; Seppänen, W.; Orho-Melander, M.; Hodson, L.; Petersen, K. F.; Shulman, G. I.; Yki-Järvinen, H. The PNPLA3 I148M Variant Increases Ketogenesis and Decreases Hepatic de Novo Lipogenesis and Mitochondrial Function in Humans. *Cell Metab.* **2023**, *35* (11), 1887-1896.e5.

(17) Imamura, F.; Fretts, A. M.; Marklund, M.; Ardisson Korat, A. V.; Yang, W. S.; Lankinen, M.; Qureshi, W.; Helmer, C.; Chen, T. A.; Virtanen, J. K.; Wong, K.; Bassett, J. K.; Murphy, R.; Tintle, N.; Yu, C. I.; Brouwer, I. A.; Chien, K. L.; Chen, Y. Y.; Wood, A. C.; del Gobbo, L. C.; Djousse, L.; Geleijnse, J. M.; Giles, G. G.; de Goede, J.; Gudnason, V.; Harris, W. S.; Hodge, A.; Hu, F.; Koulman, A.; Laakso, M.; Lind, L.; Lin, H. J.; McKnight, B.; Rajaobelina, K.; Riserus, U.; Robinson, J. G.; Samieri, C.; Senn, M.; Siscovick, D. S.; Soedamah-Muthu, S. S.; Sotoodehnia, N.; Sun, Q.; Tsai, M. Y.; Tuomainen, T. P.; Uusitupa, M.; Wagenknecht, L. E.; Wareham, N. J.; Wu, J. H. Y.; Micha, R.; Lemaitre, R. N.; Mozaffarian, D.; Forouhi, N. G. Fatty Acids in the de Novo Lipogenesis Pathway and Incidence of Type 2 Diabetes: A Pooled Analysis of Prospective Cohort Studies. *PLoS Med.* **2020**, *17* (6).

(18) Stüve, P.; Minarrieta, L.; Erdmann, H.; Arnold-Schrauf, C.; Swallow, M.; Guderian, M.; Krull, F.; Hölscher, A.; Ghorbani, P.; Behrends, J.; Abraham, W. R.; Hölscher, C.; Sparwasser, T. D.; Berod, L. De Novo Fatty Acid Synthesis during Mycobacterial Infection Is a Prerequisite for the Function of Highly Proliferative T Cells, but Not for Dendritic Cells or Macrophages. *Front. Immunol.* **2018**, *9* (APR), 1–22.

(19) Stoiber, K.; Naglo, O.; Pernpeintner, C.; Zhang, S.; Koeberle, A.; Ulrich, M.; Werz, O.; Müller, R.; Zahler, S.; Lohmüller, T.; Feldmann, J.; Braig, S. Targeting de Novo Lipogenesis as a

Novel Approach in Anti-Cancer Therapy. *Br. J. Cancer* **2018**, *118* (1), 43–51.

(20) Kampf, J. P.; Kleinfeld, A. M. Is Membrane Transport of FFA Mediated by Lipid, Protein, or Both? *Physiology* **2007**, *22* (1), 7–14.

(21) Terry, A. R.; Nogueira, V.; Rho, H.; Ramakrishnan, G.; Li, J.; Kang, S.; Pathmasiri, K. C.; Bhat, S. A.; Jiang, L.; Kuchay, S.; Cologna, S. M.; Hay, N. CD36 Maintains Lipid Homeostasis via Selective Uptake of Monounsaturated Fatty Acids during Matrix Detachment and Tumor Progression. *Cell Metab.* **2023**, *35* (11), 2060-2076.e9.

(22) Harmon, C. M.; Abumrad, N. A. Binding of Sulfosuccinimidyl Fatty Acids to Adipocyte Membrane Proteins: Isolation and Ammo-Terminal Sequence of an 88-KD Protein Implicated in Transport of Long-Chain Fatty Acids. *J. Membr. Biol.* **1993**, *133* (1), 43–49.

(23) Peche, V. S.; Pietka, T. A.; Jacome-Sosa, M.; Samovski, D.; Palacios, H.; Chatterjee-Basu, G.; Dudley, A. C.; Beatty, W.; Meyer, G. A.; Goldberg, I. J.; Abumrad, N. A. Endothelial Cell CD36 Regulates Membrane Ceramide Formation, Exosome Fatty Acid Transfer and Circulating Fatty Acid Levels. *Nat. Commun.* **2023**, *14* (1), 1–19.

(24) Endocr, I.; Agents, M.; Chem, M. The Mechanisms Linking Fatty Acid Transport To Metabolism. *Immunol. Endocr. Metab. Agents Med. Chem.* **2009**, *9* (1), 11–17.

(25) Angela, M.; Endo, Y.; Asou, H. K.; Yamamoto, T.; Tumes, D. J.; Tokuyama, H.; Yokote, K.; Nakayama, T. Fatty Acid Metabolic Reprogramming via MTOR-Mediated Inductions of PPARγ Directs Early Activation of T Cells. *Nat. Commun.* **2016**, *7*, 1–15.

(26) Madonna, M. C.; Duer, J. E.; Lee, J. V.; Williams, J.; Avsaroglu, B.; Zhu, C.; Deutsch, R.; Wang, R.; Crouch, B. T.; Hirschey, M. D.; Goga, A.; Ramanujam, N. In Vivo Optical Metabolic Imaging of Long-Chain Fatty Acid Uptake in Orthotopic Models of Triple-Negative Breast Cancer. *Cancers (Basel).* **2021**, *13* (1), 1–20.

(27) Rambold, A. S.; Cohen, S.; Lippincott-Schwartz, J. Fatty Acid Trafficking in Starved Cells: Regulation by Lipid Droplet Lipolysis, Autophagy, and Mitochondrial Fusion Dynamics. *Dev. Cell* **2015**, *32* (6), 678–692.

(28) Neef, A. B.; Schultz, C. Selective Fluorescence Labeling of Lipids in Living Cells. *Angew. Chemie - Int. Ed.* **2009**, *48* (8), 1498–1500.

(29) Hartung, K. M.; Sletten, E. M. Bioorthogonal Chemistry: Bridging Chemistry, Biology, and Medicine. *Chem* **2023**, *9* (8), 2095–2109.

(30) Howard C. Hang, John P. Wilson, G. C. Bioorthogonal Chemical Reporters for Analyzing Protein Lipidation and Lipid Trafficking. *Acc. Chem. Res.* **2011**, *44* (9), 699–708.

(31) Martin, B. R.; Cravatt, B. F. Large-Scale Profiling of Protein Palmitoylation in Mammalian Cells. *Nat. Methods* **2009**, *6* (2), 135–138.

(32) Morgan, P. K.; Huynh, K.; Pernes, G.; Miotto, P. M.; Mellett, N. A.; Giles, C.; Meikle, P. J.; Murphy, A. J.; Lancaster, G. I. Macrophage Polarization State Affects Lipid Composition and the Channeling of Exogenous Fatty Acids into Endogenous Lipid Pools. *J. Biol. Chem.* **2021**, *297* (6), 101341.

(33) Kengmo Tchoupa, A.; Peschel, A. Staphylococcus Aureus Releases Proinflammatory Membrane Vesicles To Resist Antimicrobial Fatty Acids. *mSphere* **2020**, *5* (5).

(34) Barrachina, M. N.; Pernes, G.; Becker, I. C.; Allaeys, I.; Hirsch, T. I.; Groeneveld, D. J.; Khan, A. O.; Freire, D.; Guo, K.; Carminita, E.; Morgan, P. K.; Collins, T. J. C.; Mellett, N. A.; Wei, Z.; Almazni, I.; Italiano, J. E.; Luyendyk, J.; Meikle, P. J.; Puder, M.; Morgan, N. V.; Boilard, E.;

Murphy, A. J.; Machlus, K. R. Efficient Megakaryopoiesis and Platelet Production Require Phospholipid Remodeling and PUFA Uptake through CD36. *Nat. Cardiovasc. Res.* **2023**, *2* (8), 746–763.

(35) Agard, N. J.; Prescher, J. A.; Bertozzi, C. R. A Strain-Promoted [3 + 2] Azide-Alkyne Cycloaddition for Covalent Modification of Biomolecules in Living Systems. *J. Am. Chem. Soc.* **2004**, *126* (46), 15046–15047.

(36) Oliveira, B. L.; Guo, Z.; Bernardes, G. J. L. Inverse Electron Demand Diels-Alder Reactions in Chemical Biology. *Chem. Soc. Rev.* **2017**, *46* (16), 4895–4950.

(37) Yang, J.; Šečkute, J.; Cole, C. M.; Devaraj, N. K. Live-Cell Imaging of Cyclopropene Tags with Fluorogenic Tetrazine Cycloadditions. *Angew. Chemie - Int. Ed.* **2012**, *51* (30), 7476–7479.

(38) Patterson, D. M.; Nazarova, L. A.; Xie, B.; Kamber, D. N.; Prescher, J. A. Functionalized Cyclopropenes as Bioorthogonal Chemical Reporters. *J. Am. Chem. Soc.* **2012**, *134* (45), 18638–18643.

(39) Row, R. D.; Prescher, J. A. Constructing New Bioorthogonal Reagents and Reactions. *Acc. Chem. Res.* **2018**, *51* (5), 1073–1081.

(40) Sachdeva, A.; Wang, K.; Elliott, T.; Chin, J. W. Concerted, Rapid, Quantitative, and Site-Specific Dual Labeling of Proteins. *J. Am. Chem. Soc.* **2014**, *136* (22), 7785–7788.

(41) Yu, Z.; Pan, Y.; Wang, Z.; Wang, J.; Lin, Q. Genetically Encoded Cyclopropene Directs Rapid, Photoclick-Chemistry-Mediated Protein Labeling in Mammalian Cells. *Angew. Chemie* **2012**, *124* (42), 10752–10756.

(42) Elliott, T. S.; Bianco, A.; Townsley, F. M.; Fried, S. D.; Chin, J. W. Tagging and Enriching Proteins Enables Cell-Specific Proteomics. *Cell Chem. Biol.* **2016**, *23* (7), 805–815.

(43) Elliott, T. S.; Townsley, F. M.; Bianco, A.; Ernst, R. J.; Sachdeva, A.; Elsässer, S. J.; Davis, L.; Lang, K.; Pisa, R.; Greiss, S.; Lilley, K. S.; Chin, J. W. Proteome Labeling and Protein Identification in Specific Tissues and at Specific Developmental Stages in an Animal. *Nat. Biotechnol.* **2014**, *32* (5), 465–472.

(44) Bristiel, A.; Cadinot, M.; Pizzonero, M.; Taran, F.; Urban, D.; Guignard, R.; Guianvarc'h, D. 2'-Modified Thymidines with Bioorthogonal Cyclopropene or Sydnone as Building Blocks for Copper-Free Postsynthetic Functionalization of Chemically Synthesized Oligonucleotides. *Bioconjug. Chem.* **2023**, *34* (9), 1613–1621.

(45) Eggert, F.; Kath-Schorr, S. A Cyclopropene-Modified Nucleotide for Site-Specific RNA Labeling Using Genetic Alphabet Expansion Transcription. *Chem. Commun.* **2016**, *52* (45), 7284–7287.

(46) Caulfield, C.; O'Shea, D. F.; Wu, D. Dynamic Bioorthogonal Imaging Using a Tetrazine NIR-AZA Fluorogenic Probe. *Tetrahedron* **2023**, *138*.

(47) Patterson, D. M.; Jones, K. A.; Prescher, J. A. Improved Cyclopropene Reporters for Probing Protein Glycosylation. *Mol. Biosyst.* **2014**, *10* (7), 1693–1697.

(48) Späte, A. K.; Bußkamp, H.; Niederwieser, A.; Schart, V. F.; Marx, A.; Wittmann, V. Rapid Labeling of Metabolically Engineered Cell-Surface Glycoconjugates with a Carbamate-Linked Cyclopropene Reporter. *Bioconjug. Chem.* **2014**, *25* (1), 147–154.

(49) Bertheussen, K.; van de Plassche, M.; Bakkum, T.; Gagestein, B.; Ttofi, I.; Sarris, A. J. C.; Overkleeft, H. S.; van der Stelt, M.; van Kasteren, S. I. Live-Cell Imaging of Sterculic Acid—a Naturally Occurring 1,2-Cyclopropene Fatty Acid—by Bioorthogonal Reaction with Turn-On

Tetrazine-Fluorophore Conjugates**. *Angew. Chemie* **2022**, *134* (38).

(50) Reilly, N. A.; Lutgens, E.; Kuiper, J.; Heijmans, B. T.; Wouter Jukema, J. Effects of Fatty Acids on T Cell Function: Role in Atherosclerosis. *Nat. Rev. Cardiol.* **2021**, *18* (12), 824–837.

(51) Jones, R. G.; Thompson, C. B. Revving the Engine: Signal Transduction Fuels T Cell Activation. *Immunity* **2007**, *27* (2), 173–178.

(52) Nunn, J. R. The Structure of Sterculic Acid. *J. Chem. Soc.* **1952**, 313–318.

(53) Hernando, J.; Matía, M. P.; Novella, J. L.; Alvarez-Builla, J. Synthesis of Sterculic Acid. *Arkivoc* **2002**, *2002* (5), 27–30.

(54) Gensler, W. J.; Floyd, M. B.; Yanase, R.; Pober, K. W. Synthesis of Methyl Sterculate. *J. Am. Chem. Soc.* **1970**, *92* (8), 2472–2475.

(55) N.T. Castellucci, C. E. G. Synthesis of Sterculic Acid. *J. Am. Chem. Soc.* **1960**, *82* (15), 4107–4107.

(56) Gensler, W. J.; Poser, K. W.; Solomon, D. M.; Floyd, B. Synthesis of Methyl Malvalate and Methyl 5,6-Methano-5-Undecenoate. *J. Org. Chem.* **1970**, *35* (7), 2301–2307.

(57) Adams, J.; Spero, D. M. Rhodium (II) Catalyzed Reactions of Diazo-Carbonyl Compounds. *Tetrahedron* **1991**, *47* (10–11), 1765–1808.

(58) Ando, T.; Ohno, R.; Ikemoto, K.; Yajima, Y. Cyclopropene Fatty Acid and Amide: Inhibitors of the Pheromone Biosynthesis in Bombyx Mori. *J. Pestic. Sci.* **1995**, *20* (1), 25–32.

(59) Al Dulayymi, A. R.; Al Dulayymi, J. R.; Baird, M. S.; Gerrard, M. E.; Koza, G.; Harkins, S. D.; Roberts, E. 1,2,2-Tribromocyclopropanecarboxylic Acid and Derivatives - Valuable Intermediates for Four Carbon Cyclopropane and Cyclopropene Synthons. *Tetrahedron* **1996**, *52* (10), 3409–3424.

(60) Baird, M. S.; Dale, C. M.; Lytollis, W.; Simpson, M. J. A New Approach to Cyclopropene Fatty Acids. *Tetrahedron Lett.* **1992**, *33* (11), 1521–1522.

(61) House, S. Wittig Olefination Reaction. *Chem. Rev.* **1989**, 863–927.

(62) Oger, C.; Balas, L.; Durand, T.; Galano, J. M. Are Alkyne Reductions Chemo-, Regio-, and Stereoselective Enough to Provide Pure (Z)-Olefins in Polyfunctionalized Bioactive Molecules? *Chem. Rev.* **2013**, *113* (3), 1313–1350.

(63) Wetherill, R. B.; Brown, C. The Reaction of Sodium Borohydride with Nickel Acetate in Ethanol Solution – a Highly Selective Nickel Hydrogenation Catalyst. *J. Am. Chem. Soc.* **1963**, *85* (7), 1005–1006.

(64) Brown, C. A.; Ahuja, V. K. Catalytic Hydrogenation. VI. The Reaction of Sodium Borohydride with Nickel Salts in Ethanol Solution. P-2 Nickel, a Highly Convenient, New, Selective Hydrogenation Catalyst with Great Sensitivity to Substrate Structure. *J. Org. Chem.* **1973**, *38* (12), 2226–2230.

(65) Hidalgo, M. A.; Carretta, M. D.; Burgos, R. A. Long Chain Fatty Acids as Modulators of Immune Cells Function: Contribution of FFA1 and FFA4 Receptors. *Front. Physiol.* **2021**, *12* (July), 1–18.

(66) Almeida, L.; Everts, B. Fa(c)t Checking: How Fatty Acids Shape Metabolism and Function of Macrophages and Dendritic Cells. *Eur. J. Immunol.* **2021**, *51* (7), 1628–1640.

(67) Pelgrom, L. R.; Davis, G. M.; O'Shaughnessy, S.; Wezenberg, E. J. M.; Van Kasteren, S. I.; Finlay, D. K.; Sinclair, L. V. QUAS-R: An SLC1A5-Mediated Glutamine Uptake Assay with Single-Cell Resolution Reveals Metabolic Heterogeneity with Immune Populations. *Cell Rep.* **2023**, *42*

(8), 112828.

(68) Pelgrom, L. R.; Patente, T. A.; Otto, F.; Nouwen, L. V.; Ozir-Fazalalikhan, A.; van der Ham, A. J.; van der Zande, H. J. P.; Heieis, G. A.; Arens, R.; Everts, B. MTORC1 Signaling in Antigen-Presenting Cells of the Skin Restrains CD8+ T Cell Priming. *Cell Rep.* **2022**, *40* (1), 111032.

(69) Fan, H.; Xia, S.; Xiang, J.; Li, Y.; Ross, M. O.; Lim, S. A.; Yang, F.; Tu, J.; Xie, L.; Dougherty, U.; Zhang, F. Q.; Zheng, Z.; Zhang, R.; Wu, R.; Dong, L.; Su, R.; Chen, X.; Althaus, T.; Riedell, P. A.; Jonker, P. B.; Muir, A.; Lesinski, G. B.; Rafiq, S.; Dhodapkar, M. V.; Stock, W.; Odenike, O.; Patel, A. A.; Opferman, J.; Tsuji, T.; Matsuzaki, J.; Shah, H.; Faubert, B.; Elf, S. E.; Layden, B.; Bissonnette, B. M.; He, Y. Y.; Kline, J.; Mao, H.; Odunsi, K.; Gao, X.; Chi, H.; He, C.; Chen, J. Trans-Vaccenic Acid Reprograms CD8+ T Cells and Anti-Tumour Immunity. *Nature* **2023**, *623* (7989), 1034–1043.

(70) Laval, T.; Demangel, C. Click-Chemistry-Based Protocol to Quantitatively Assess Fatty Acid Uptake by Mycobacterium Tuberculosis in Axenic Culture and inside Mouse Macrophages. *STAR Protoc.* **2023**, *4* (1), 102062.

(71) Huh, H.; Pearce, S.; Yesner, L.; Schindler, J.; Silverstein, R. Regulated Expression of CD36 during Monocyte-to-Macrophage Differentiation: Potential Role of CD36 in Foam Cell Formation. *Blood* **1996**, *87* (5), 2020–2028.

(72) Savina, A.; Amigorena, S. Phagocytosis and Antigen Presentation in Dendritic Cells. *Immunol. Rev.* **2007**, *219* (1), 143–156.

(73) Eisenbarth, S. C. Dendritic Cell Subsets in T Cell Programming: Location Dictates Function. *Nat. Rev. Immunol.* **2019**, *19* (2), 89–103.

(74) Guria, S.; Daniliuc, C. G.; Hennecke, U. Brønsted Acid-Catalyzed Enantioselective Iodocycloetherification Enabled by Triphenylphosphine Selenide Cocatalysis. *Adv. Synth. Catal.* **2021**, *363* (15), 3852–3858.

(75) Al Dulayymi, J. R.; Baird, M. S.; Simpson, M. J.; Nyman, S.; Port, G. R. Structure Based Interference with Insect Behaviour - Cyclopropene Analogues of Pheromones Containing Z-Alkenes. *Tetrahedron* **1996**, *52* (38), 12509–12520.

(76) Gung, B. W.; Omollo, A. O. First Total Synthesis of the Potent Anticancer Natural Product Dideoxypetrosynol A: Preparation of the “Skipped” (Z)-Enediyne Moiety by Oxidative Coupling of Homopropargylphosphonium Ylide. *European J. Org. Chem.* **2008**, No. 28, 4790–4795.

(77) Lin, L.; Zhao, Q.; Li, A. N.; Ren, F.; Yang, F.; Wang, R. Enantioselective Synthesis of Anomala Osakana Pheromone and Janus Integer Pheromone: A Flexible Approach to Chiral γ-Butyrolactones. *Org. Biomol. Chem.* **2009**, *7* (18), 3663–3665.

(78) Tasdemir, D.; Sanabria, D.; Lauinger, I. L.; Tarun, A.; Herman, R.; Perozzo, R.; Zloh, M.; Kappe, S. H.; Brun, R.; Carballeira, N. M. 2-Hexadecynoic Acid Inhibits Plasmodial FAS-II Enzymes and Arrests Erythrocytic and Liver Stage Plasmodium Infections. *Bioorganic Med. Chem.* **2010**, *18* (21), 7475–7485.

(79) Sydnes, L. K.; Bakstad, E. Formation of Acetylenic Acetals by Ring Opening of 1,1,2-Trihalocyclopropanes under Phase-Transfer Conditions. *Acta Chemica Scandinavica*. 1996, pp 446–453.

(80) Crawford, P. J. K. and S. D. Surface-Mediated Reactions. 4. Hydrohalogenation of Alkynes. *J. Org. Chem.* **1994**, *59*, 3102–3112.

(81) Baumann, A. N.; Music, A.; Karaghiosoff, K.; Didier, D. Highly Diastereoselective Approach to Methylenecyclopropanes via Boron-Homologation/Allylboration Sequences. *Chem. Commun.* **2016**, *52* (12), 2529–2532.

(82) Winter, A. J.; Rowe, M. T.; Weir, A. N. M.; Akter, N.; Mbatha, S. Z.; Walker, P. D.; Williams, C.; Song, Z.; Race, P. R.; Willis, C. L.; Crump, M. P. Programmed Iteration Controls the Assembly of the Nonanoic Acid Side Chain of the Antibiotic Mupirocin. *Angew. Chemie - Int. Ed.* **2022**, *61* (50), 1–10.

(83) Fortunati, T.; D'Acunto, M.; Caruso, T.; Spinella, A. Chemoenzymatic Preparation of Musky Macrolactones. *Tetrahedron* **2015**, *71* (16), 2357–2362.

(84) Dunny, E.; Evans, P. Stereocontrolled Synthesis of the PPAR-γ Agonist 10-Nitrolinoleic Acid. *J. Org. Chem.* **2010**, *75* (15), 5334–5336.

(85) Offenbacher, A. R.; Zhu, H.; Klinman, J. P. Synthesis of Site-Specifically13C Labeled Linoleic Acids. *Tetrahedron Lett.* **2016**, *57* (41), 4537–4540.

(86) Serhan, M.; Sprowls, M.; Jackemeyer, D.; Long, M.; Perez, I. D.; Maret, W.; Tao, N.; Forzani, E. Total Iron Measurement in Human Serum with a Smartphone. *Org. Biomol. Chem.* **2017**, *15* (20), 4308–4313.

(87) Tanabe, Shuhei; Kobayashi, Y. Synthesis of Resolvin E3 via Palladium-Catalyzed Addition of AcOH to Vinyl Epoxy Alcohols. *Org. Biomol. Chem.* **2019**, *17* (9), 2393–2402.

(88) Peng, S.; Okeley, N. M.; Tsai, A. L.; Wu, G.; Kulmacz, R. J.; Van der Donk, W. A. Synthesis of Isotopically Labeled Arachidonic Acids to Probe the Reaction Mechanism of Prostaglandin H Synthase. *J. Am. Chem. Soc.* **2002**, *124* (36), 10785–10796.

(89) Jiang, X.; Zhang, J.; Ma, S. Iron Catalysis for Room-Temperature Aerobic Oxidation of Alcohols to Carboxylic Acids. *J. Am. Chem. Soc.* **2016**, *138* (27), 8344–8347.

(90) Thurnhofer, S.; Vetter, W. Synthesis of (S)-(+)-Enantiomers of Food-Relevant (n-5)-Monoenoic and Saturated Anteiso-Fatty Acids by a Wittig Reaction. *Tetrahedron* **2007**, *63* (5), 1140–1145.

(91) Rafferty, S. M.; Rutherford, J. E.; Zhang, L.; Wang, L.; Nagib, D. A. Cross-Selective Aza-Pinacol Coupling via Atom Transfer Catalysis. *J. Am. Chem. Soc.* **2021**, *143* (15), 5622–5628.

(92) Rui, F.; Boland, W. Algal Pheromone Biosynthesis: Stereochemical Analysis and Mechanistic Implications in Gametes of Ectocarpus Siliculosus. *J. Org. Chem.* **2010**, *75* (12), 3958–3964.